

Observation of multi-ten TeV to sub-PeV gamma rays from the HESS J1843-033 region with the Tibet air shower array

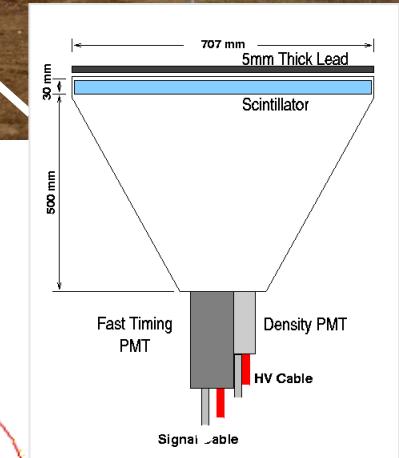
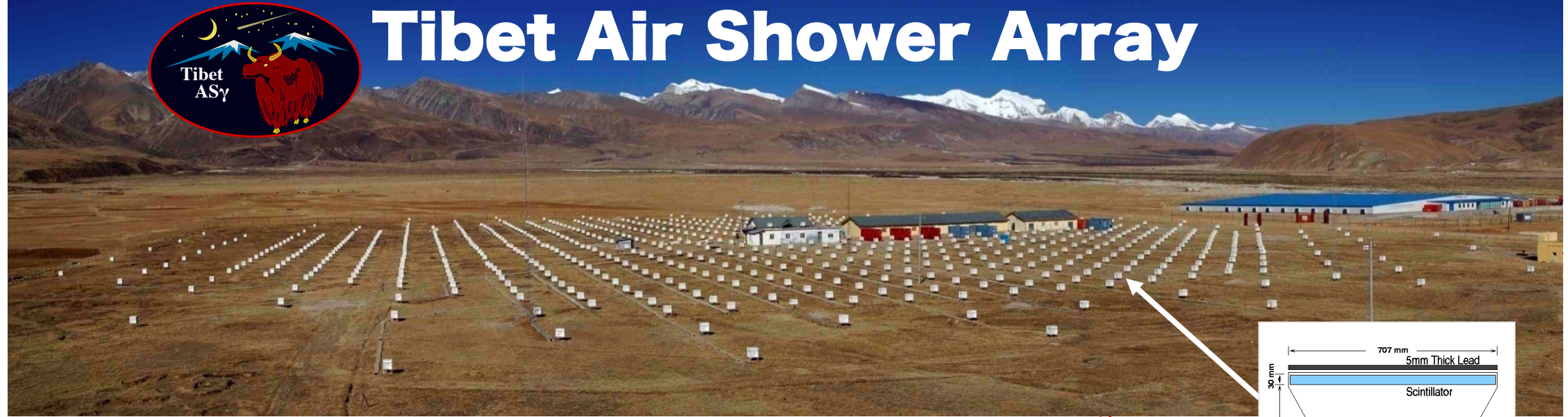
Kato Sei (ICRR) for the Tibet AS γ collaboration

This presentation is based on

“Measurement of the Gamma-Ray Energy Spectrum beyond 100 TeV from the HESS J1843-033 Region”,
Amenomori et al., ApJ 932, 120 (2022) published online
(<https://doi.org/10.3847/1538-4357/ac6ef4>)

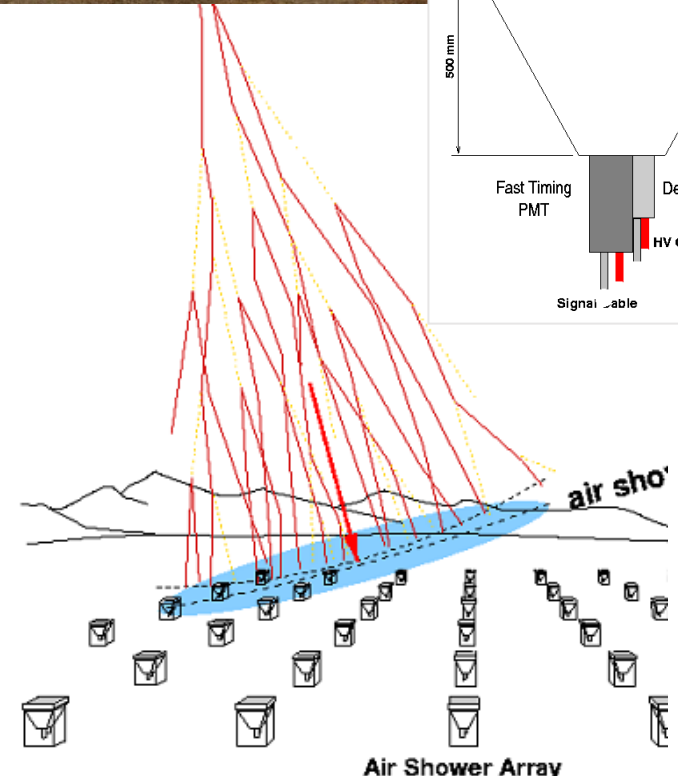


Tibet Air Shower Array



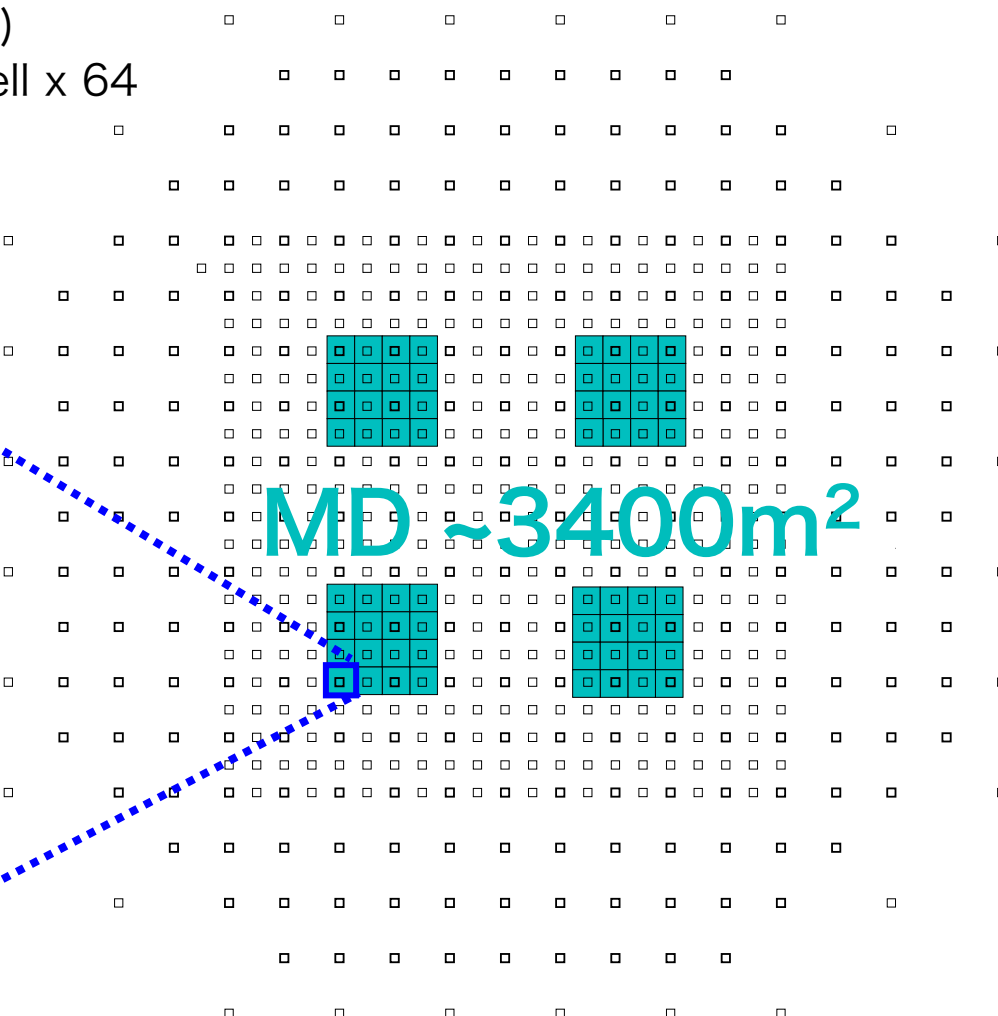
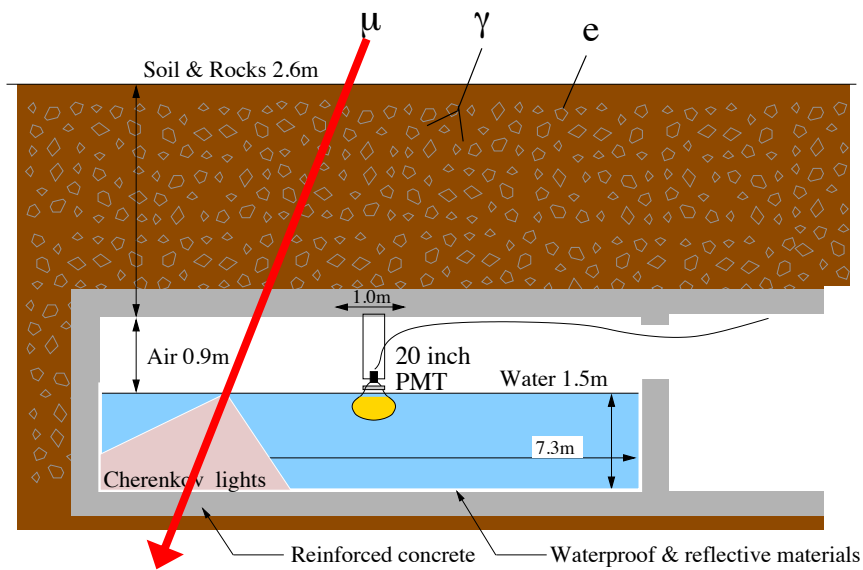
- Tibet, China (90.522°E , 30.102°N) 4,300 m a.s.l.
- scintillation counters $0.5 \text{ m}^2 \times 597$
- area $\sim 65,700 \text{ m}^2$
- angular resolution (gamma rays) $\sim 0.5^{\circ} @ 10\text{TeV}$
 $\sim 0.2^{\circ} @ 100\text{TeV}$
- energy resolution (gamma rays) $\sim 40\% @ 10\text{TeV}$
 $\sim 20\% @ 100\text{TeV}$

2nd particles timing → arrival direction
2nd particles energy deposit → primary energy



Water Cherenkov Muon Detector Array

- ✓ 2.4m underground ($515\text{g/cm}^2 \sim 19X_0$)
- ✓ $7.35\text{m} \times 7.35\text{m} \times 1.5\text{m}$ -deep water cell $\times 64$
- ✓ 20"ΦPMT (HAMAMATSU R3600)
- ✓ Concrete pools + Tyvek sheets



Measurement of number of muons in air showers
→ γ/CR discrimination



Tibet AS γ Collaboration



M. Amenomori¹, S. Asano², Y. W. Bao³, X. J. Bi⁴, D. Chen⁵, T. L. Chen⁶, W. Y. Chen⁴, Xu Chen^{4,5}, Y. Chen³, Cirennima⁶, S. W. Cui⁷, Danzengluobu⁶, L. K. Ding⁴, J. H. Fang^{4,8}, K. Fang⁴, C. F. Feng⁹, Zhaoyang Feng⁴, Z. Y. Feng¹⁰, Qi Gao⁶, A. Gomi¹¹, Q. B. Gou⁴, Y. Q. Guo⁴, Y. Y. Guo⁴, Y. Hayashi², H. H. He⁴, Z. T. He⁷, K. Hibino¹², N. Hotta¹³, Haibing Hu⁶, H. B. Hu⁴, K. Y. Hu^{4,8}, J. Huang⁴, H. Y. Jia¹⁰, L. Jiang⁴, P. Jiang⁵, H. B. Jin⁵, K. Kasahara¹⁴, Y. Katayose¹¹, C. Kato², S. Kato¹⁵, I. Kawahara¹¹, T. Kawashima¹⁵, K. Kawata¹⁵, M. Kozai¹⁶, D. Kurashige¹¹, Labaciren⁶, G. M. Le¹⁷, A. F. Li^{4,9,18}, H. J. Li⁶, W. J. Li^{4,10}, Y. Li⁵, Y. H. Lin^{4,8}, B. Liu¹⁹, C. Liu⁴, J. S. Liu⁴, L. Y. Liu⁵, M. Y. Liu⁶, W. Liu⁴, X. L. Liu⁵, Y.-Q. Lou^{20,21,22}, H. Lu⁴, X. R. Meng⁶, Y. Meng^{4,8}, K. Munakata², K. Nagaya¹¹, Y. Nakamura¹⁵, Y. Nakazawa²³, H. Nanjo¹, C. C. Ning⁶, M. Nishizawa²⁴, R. Noguchi¹¹, M. Ohnishi¹⁵, S. Okukawa¹¹, S. Ozawa²⁵, L. Qian⁵, X. Qian⁵, X. L. Qian²⁶, X. B. Qu²⁷, T. Saito²⁸, Y. Sakakibara¹¹, M. Sakata²⁹, T. Sako¹⁵, T. K. Sako¹⁵, T. Sasaki¹², J. Shao^{4,9}, M. Shibata¹¹, A. Shiomi²³, H. Sugimoto³⁰, W. Takano¹², M. Takita¹⁵, Y. H. Tan⁴, N. Tateyama¹², S. Torii³¹, H. Tsuchiya³², S. Udo¹², H. Wang⁴, Y. P. Wang⁶, Wangdui⁶, H. R. Wu⁴, Q. Wu⁶, J. L. Xu⁵, L. Xue⁹, Z. Yang⁴, Y. Q. Yao⁵, J. Yin⁵, Y. Yokoe¹⁵, N. P. Yu⁵, A. F. Yuan⁶, L. M. Zhai⁵, C. P. Zhang⁵, H. M. Zhang⁴, J. L. Zhang⁴, X. Zhang³, X. Y. Zhang⁹, Y. Zhang⁴, Yi Zhang³³, Ying Zhang⁴, S. P. Zhao⁴, Zhaxisangzhu⁶, X. X. Zhou¹⁰ and Y. H. Zou^{4,8}

1 Department of Physics, Hirosaki Univ., Japan.

2 Department of Physics, Shinshu Univ., Japan.

3 School of Astronomy and Space Science, Nanjing Univ., China.

4 Key Laboratory of Particle Astrophysics, Institute of High Energy Physics, CAS, China.

5 National Astronomical Observatories, CAS, China.

6 Department of Mathematics and Physics, Tibet Univ., China.

7 Department of Physics, Hebei Normal Univ., China.

8 Univ. of Chinese Academy of Sciences, China.

9 Institute of Frontier and Interdisciplinary Science and Key Laboratory of Particle Physics and Particle Irradiation (MOE), Shandong Univ., China.

10 Institute of Modern Physics, SouthWest Jiaotong Univ., China.

11 Faculty of Engineering, Yokohama National Univ., Japan.

12 Faculty of Engineering, Kanagawa Univ., Japan.

13 Faculty of Education, Utsunomiya Univ., Japan.

14 Faculty of Systems Engineering, Shibaura Institute of Technology, Japan.

15 Institute for Cosmic Ray Research, Univ. of Tokyo, Japan.

16 Polar Environment Data Science Center, Joint Support-Center for Data Science Research, Research Organization of Information and Systems, Japan.

17 National Center for Space Weather, China Meteorological Administration, China.

18 School of Information Science and Engineering, Shandong Agriculture Univ., China.

19 Department of Astronomy, School of Physical Sciences, Univ. of Science and Technology of China, China.

20 Department of Physics and Tsinghua Centre for Astrophysics (THCA), Tsinghua Univ., China.

21 Tsinghua Univ.-National Astronomical Observatories of China (NAOC) Joint Research Center for Astrophysics, Tsinghua Univ., China.

22 Department of Astronomy, Tsinghua Univ., China.

23 College of Industrial Technology, Nihon Univ., Japan.

24 National Institute of Informatics, Japan.

25 National Institute of Information and Communications Technology, Japan.

26 Department of Mechanical and Electrical Engineering, Shandong Management Univ., China.

27 College of Science, China Univ. of Petroleum, China.

28 Tokyo Metropolitan College of Industrial Technology, Japan.

29 Department of Physics, Konan Univ., Japan.

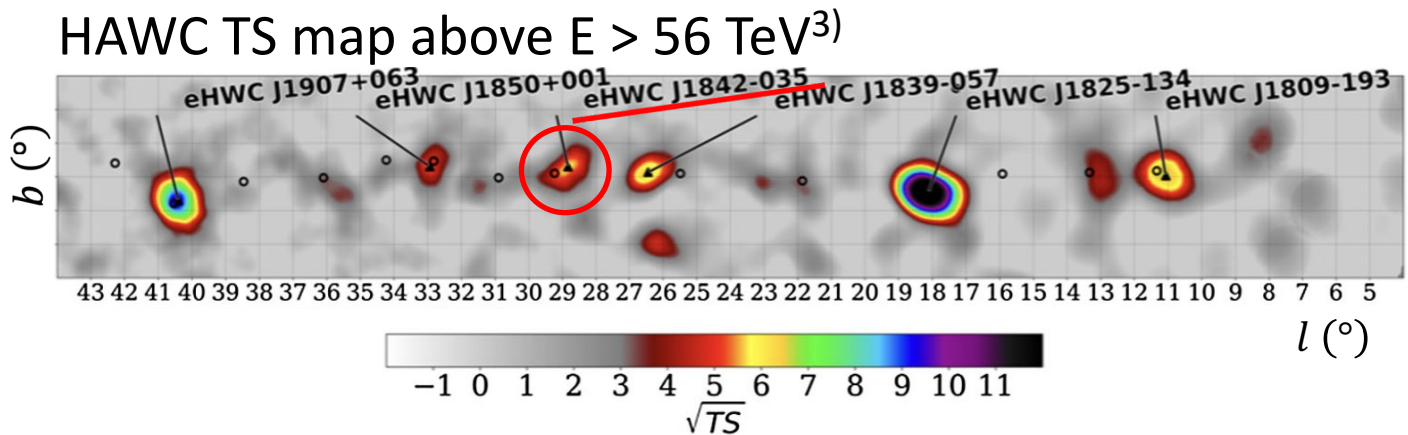
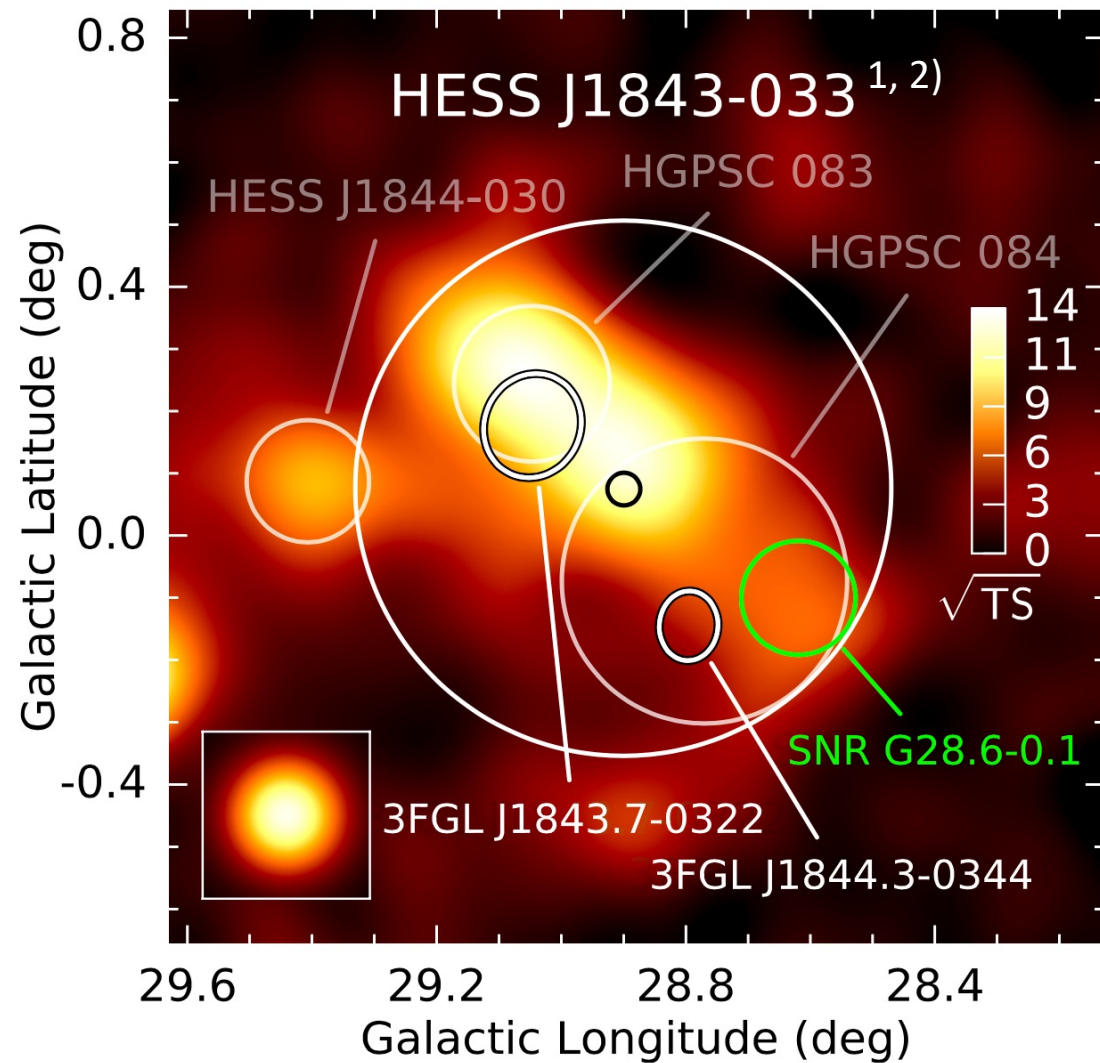
30 Shonan Institute of Technology, Japan.

31 Research Institute for Science and Engineering, Waseda Univ., Japan.

32 Japan Atomic Energy Agency, TJapan.

33 Key Laboratory of Dark Matter and Space Astronomy, Purple Mountain Observatory, CAS, China.

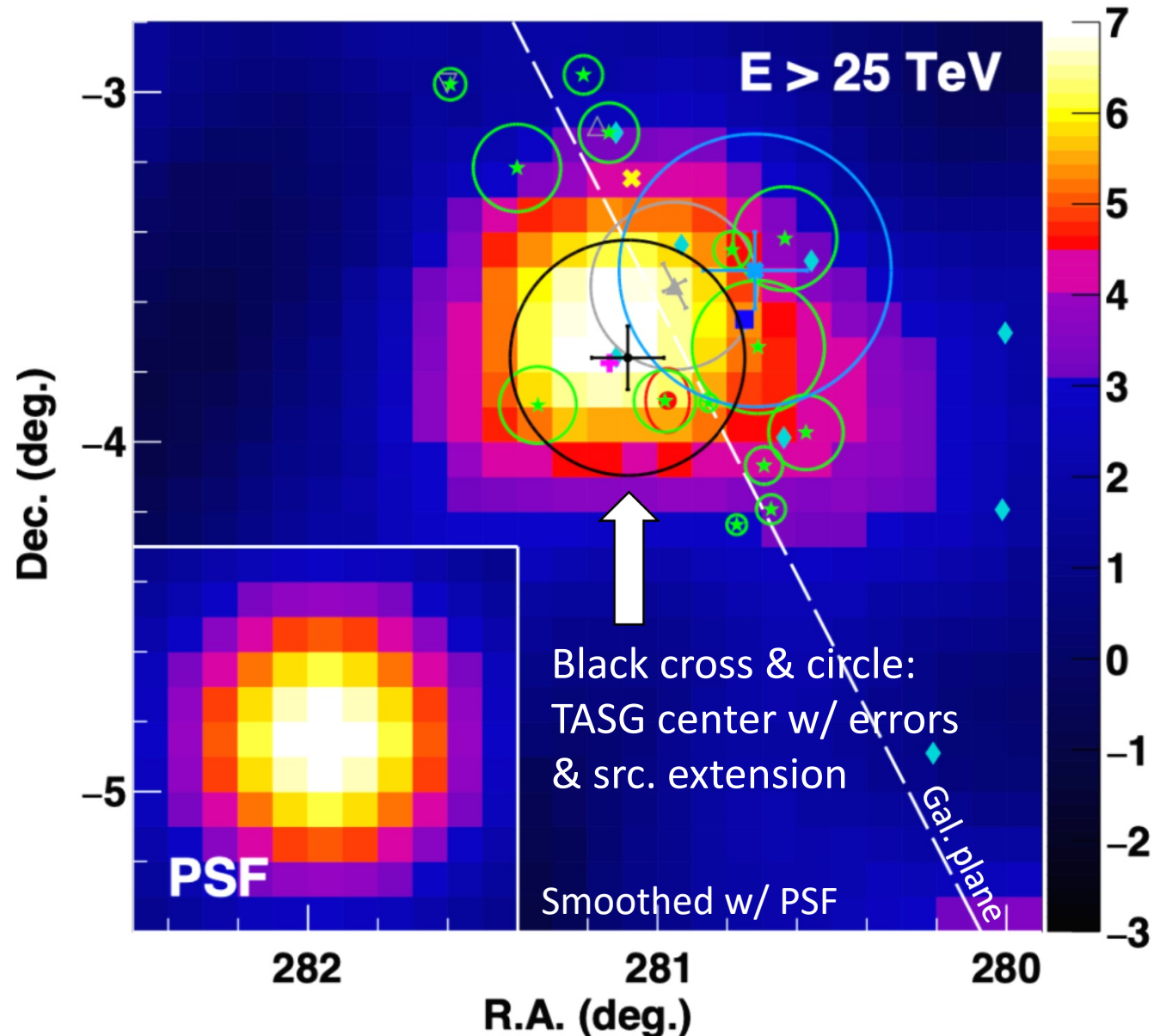
HESS J1843-033: Unidentified TeV gamma-ray source



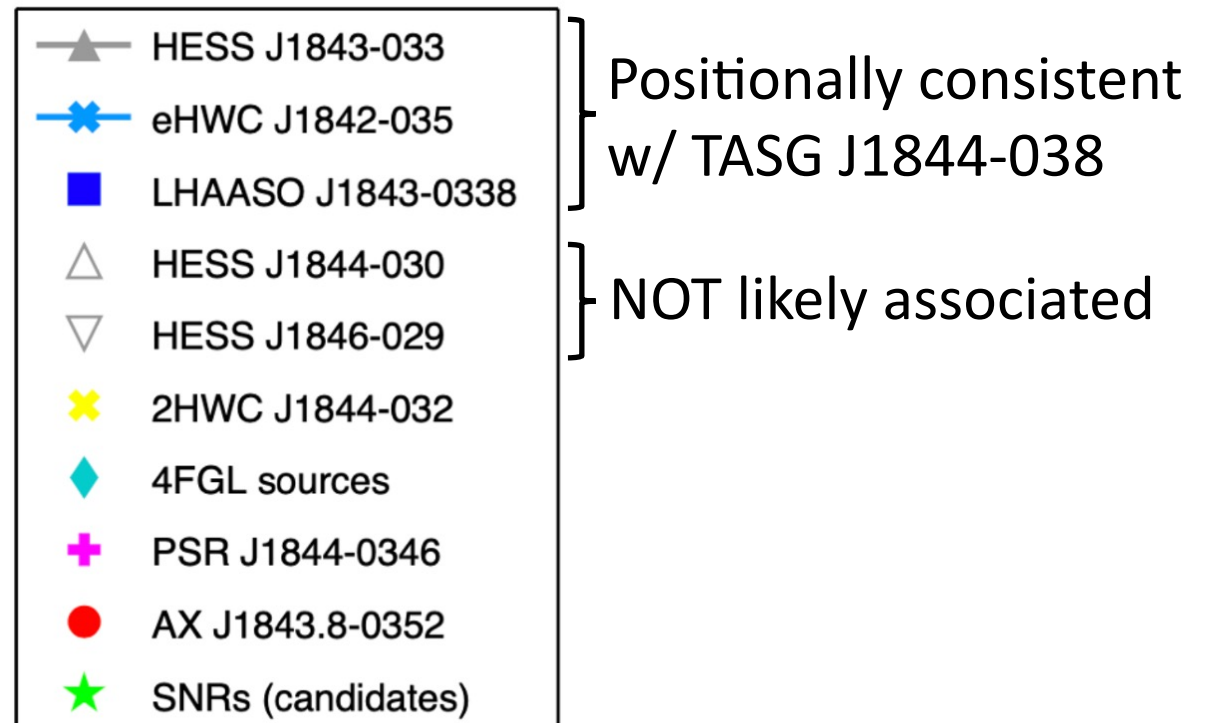
- Nearby gamma-ray sources:
 - eHWC J1842-035³⁾ in $E > 56 \text{ TeV}$ &
 - LHAASO J1843-033⁸⁴⁾ @ $E = 100 \text{ TeV}$
- Gamma-ray emission mechanism is not known
- Energy spectrum is not measured above 30 TeV

- 1) Hoppe, Proc. of ICRC 2007 (2008)
- 2) H.E.S.S. collaboration, A&A 612, A1 (2018)
- 3) Abeysekara et al., PRL 124, 021102 (2020)
- 4) Cao et al., Nature, 594, 3 (2021)

Results (1): Source detection: TASG J1844-038

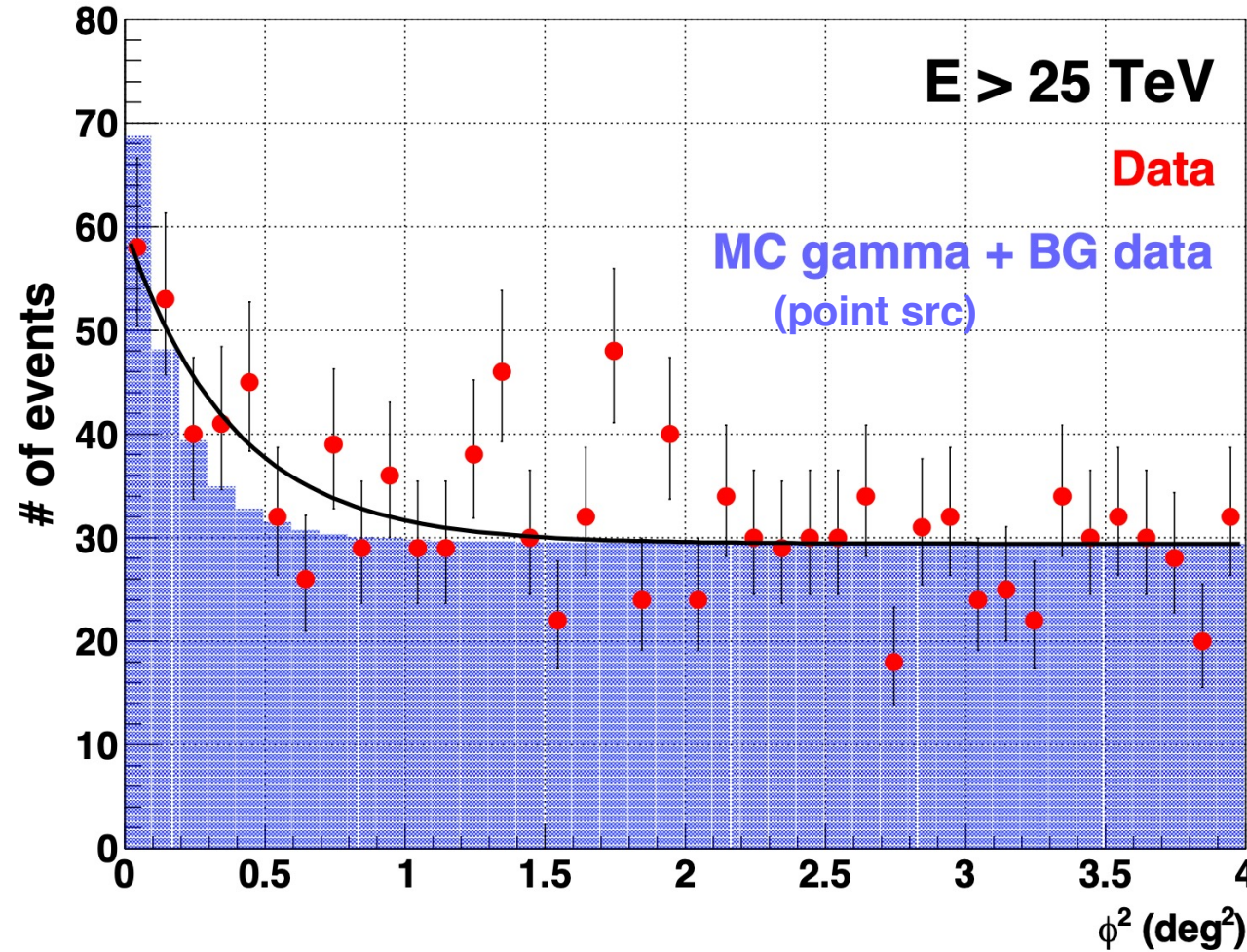


- Used data: 2014 Feb. to 2017 May (719 live days)
- Li & Ma¹⁾ significance: 6.2σ ($E > 25$ TeV)
- Source center in the J2000 coordinates: $(\alpha, \delta) = (281^\circ 09 \pm 0^\circ 10, -3^\circ 76 \pm 0^\circ 09)$



Results (2): ϕ^2 distribution of the TASG J1844-038 region

ϕ^2 : The square of the angle b/w the source center and incoming direction of events



$$G(\phi^2; A, \sigma_{\text{ext}}) = A \exp\left(-\frac{\phi^2}{2(\sigma_{\text{ext}}^2 + \sigma_{\text{psf}}^2)}\right) + N_{\text{bg}}$$

where $\sigma_{\text{psf}} = 0.28^\circ$: PSF radius and

$N_{\text{bg}} = 29.4$: # of BG.

⇒ Source extension: $\sigma_{\text{ext}} = 0.34^\circ \pm 0.12^\circ$

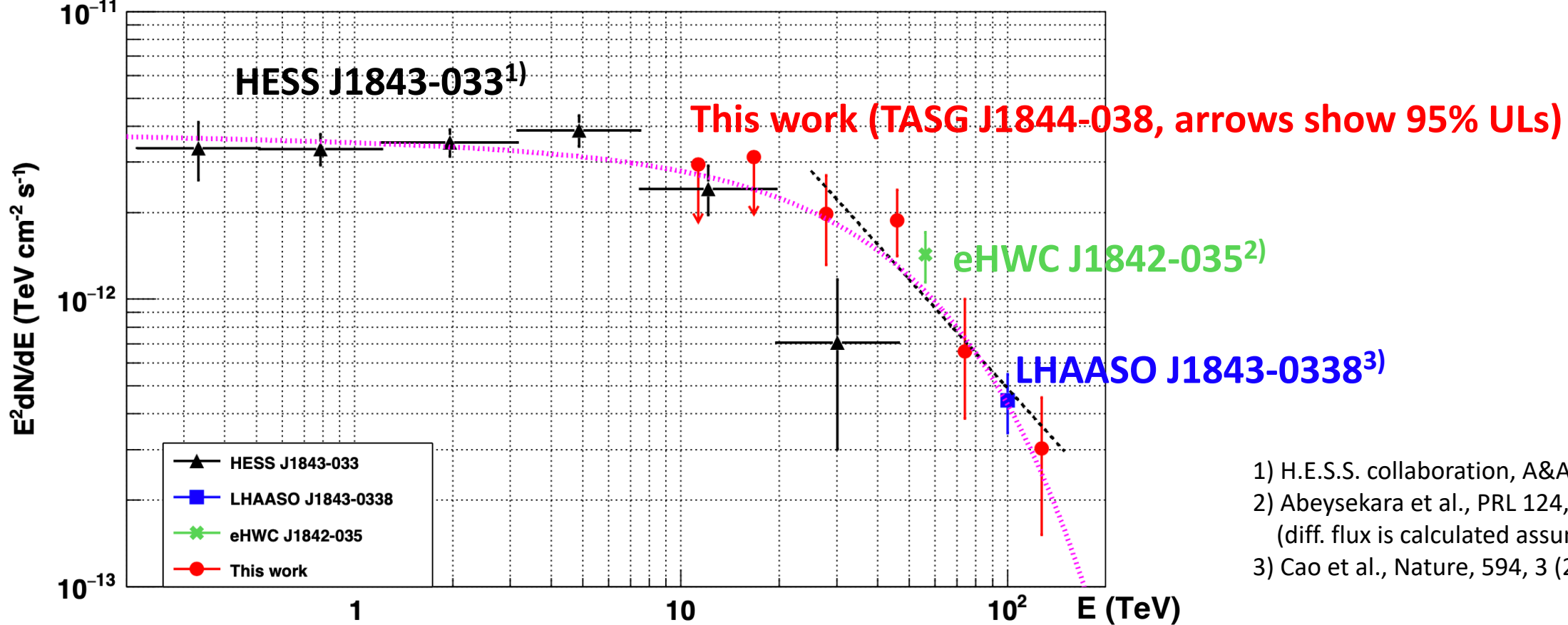
$(\chi^2 / \text{d.o.f.} = 39.5 / 38)$

The extension is consistent w/
HESS J1843-033¹⁾: $0.24^\circ \pm 0.06^\circ$ ($E > 400$ GeV) &
eHWC J1842-035²⁾: $0.39^\circ \pm 0.09^\circ$ ($E > 56$ TeV).

1) H.E.S.S. collaboration, A&A 612, A1 (2018)

2) Abeysekara et al., PRL 124, 021102 (2020)

Results (3): Energy spectrum



1) H.E.S.S. collaboration, A&A 612, A1 (2018)

2) Abeysekara et al., PRL 124, 021102 (2020)
(diff. flux is calculated assuming $\Gamma=2.7$)

3) Cao et al., Nature, 594, 3 (2021)

PL fit to this work
(Black dashed in $25 \text{ TeV} < E < 130 \text{ TeV}$)

$$: \frac{dN}{dE} = (9.70 \pm 1.89) \times 10^{-16} \left(\frac{E}{40 \text{ TeV}} \right)^{-3.26 \pm 0.30} \text{ TeV}^{-1} \text{ cm}^{-2} \text{ s}^{-1} \\ (\chi^2/\text{d. o. f.} = 2.1/2)$$

ECPL fit to HESS, LHAASO & this work:
(Magenta dotted)

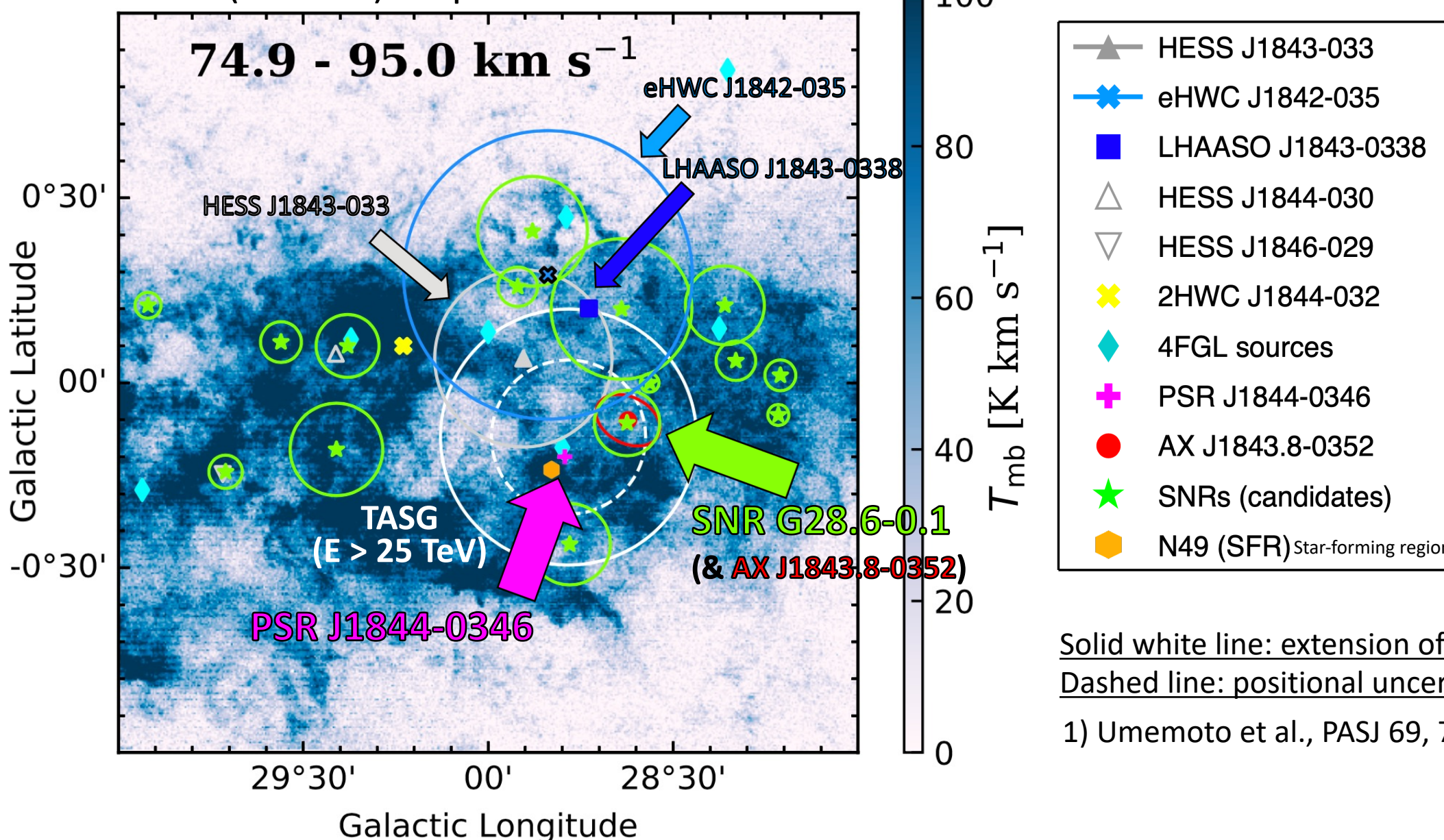
$$\frac{dN}{dE} = N_0 \left(\frac{E}{\text{TeV}} \right)^{-\Gamma} \exp \left(-\frac{E}{E_{\text{cut}}} \right)$$

$$\text{where } N_0 = (3.57 \pm 0.26) \times 10^{-12} \text{ TeV}^{-1} \text{ cm}^{-2} \text{ s}^{-1},$$

$$\Gamma = 2.02 \pm 0.06 \text{ & } E_{\text{cut}} = 49.5 \pm 9.0 \text{ TeV } (\chi^2/\text{d. o. f.} = 10.4/8).$$

Discussion: Association of TASG J1844-038 w/ nearby objects

12CO ($J = 1 - 0$) map from the FUGIN data¹⁾



Discussion (1): Association of TASG J1844-038 w/ SNR G28.6-0.1 (1)

SNR G28.6-0.1

- Nonthermal radio¹⁾ & X-rays²⁾ by electron synchrotron radiation
- Shell-type SNR²⁾
- Distance: 9.6 ± 0.3 kpc³⁾
- Age: 2.7 kyr²⁾ or 19 kyr³⁾

TASG J1844-038's radius: $\sigma = 0.34^\circ \pm 0.12^\circ$

AX J1843.8-0352's radius (X-rays): $\sigma_{\text{mean}} = 4.5' \text{ }^4)$

Discrepancy in their extensions at the 2.3σ level

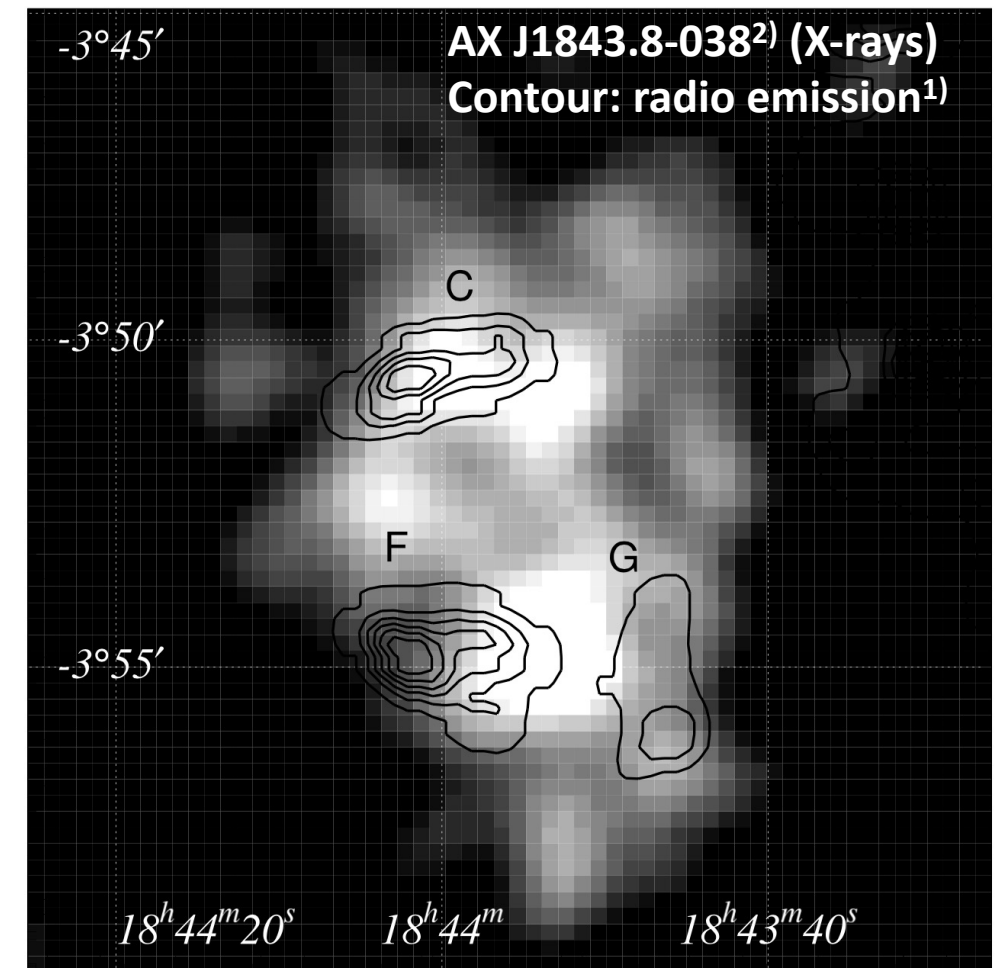
=> Contribution of gamma ray of hadronic origin ?
(CR interaction w/ ambient molecular clouds ?)

1) Helfand et al., ApJ 341, 151 (1989)

2) Bamba et al., PASJ 53, L21 (2001)

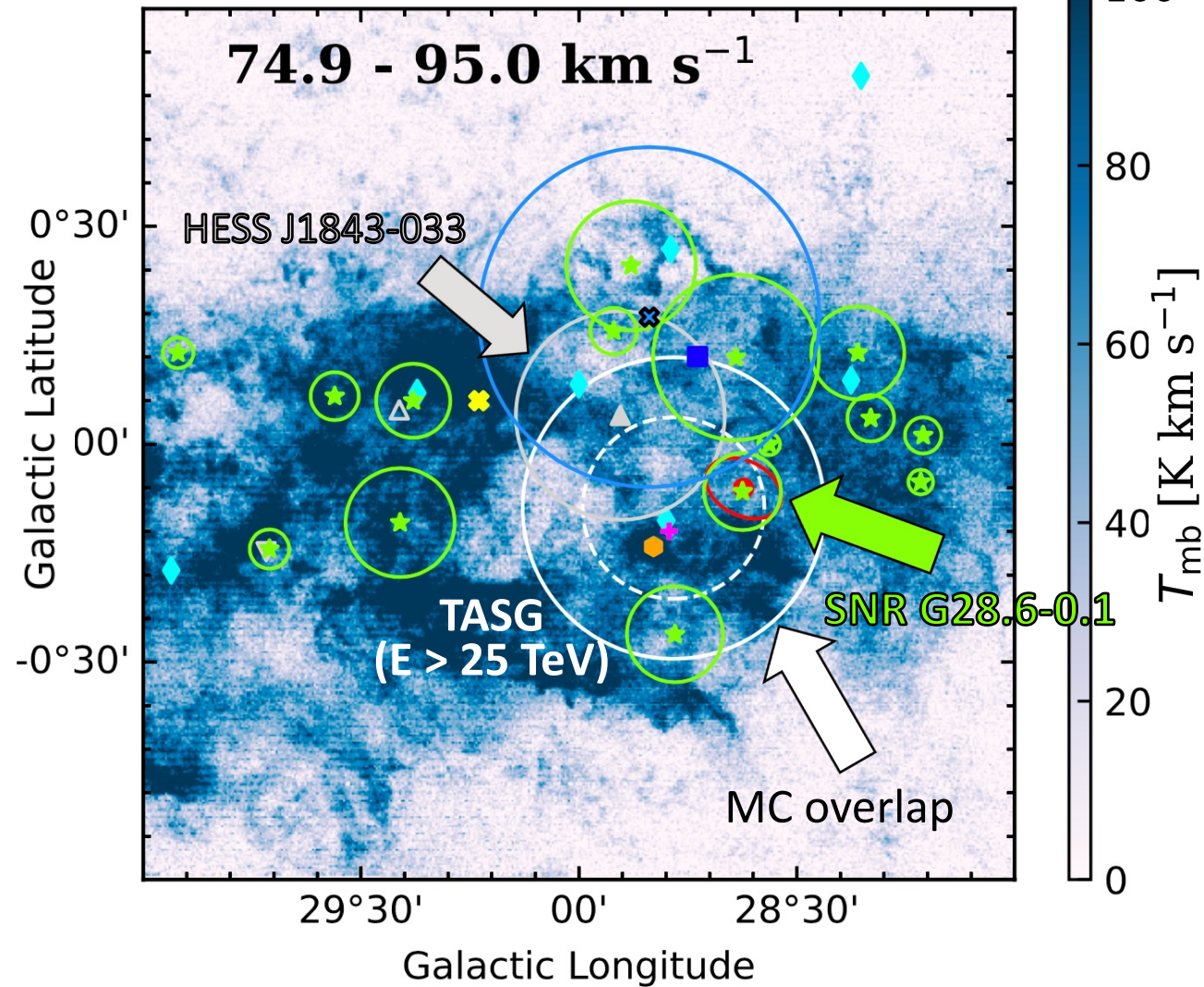
3) Ranasinghe & Leahy, MNRAS 477, 2243 (2018)

4) Ueno et al., ApJ 588, 338 (2003)



Discussion (1): Association of TASG J1844-038 w/ SNR G28.6-0.1 (2)

12CO ($J = 1 - 0$) map from the FUGIN data¹⁾



Several resemblances to SNR G106.3+2.7²⁾:

1. Overlapping molecular clouds (MCs),
2. Max. energy of CR protons: $\simeq 500\text{TeV}$, &
3. Average of the estimated ages is $\simeq 10 \text{ kyr}$.

=> Could have been a PeVatron in the past??

Diffusion time of CR protons through MCs³⁾:

$$\tau_{\text{diff}} = \frac{R_{\text{cl}}^2}{6D(E)} \sim 1.2 \cdot 10^4 \chi^{-1} \left(\frac{R_{\text{tot}}}{20 \text{ pc}} \right)^2 \left(\frac{E}{\text{GeV}} \right)^{-0.5} \left(\frac{B}{10 \mu\text{G}} \right)^{0.5} \text{yr}$$

where R, size of MCs & χ , suppression factor.

Assuming $\chi = 0.1$ & $B = 10 \mu\text{G}$ ($n_{\text{H}} \sim 100 \text{ cm}^{-3}$),

$\tau_{\text{diff}} (R_{\text{TASG}}, E_{\text{CR}} > 250 \text{ TeV}) \lesssim 2.0 \text{ kyr}$ &

$\tau_{\text{diff}} (R_{\text{HESS}}, E_{\text{CR}} \simeq 10 \text{ TeV}) \simeq 4.9 \text{ kyr}$.

Acceptable compared w/ the SNR's age

1) Umemoto et al., PASJ 69, 78 (2017)

2) Amenomori et al., Nat. Astron. 5, 460 (2021)

3) Gabici et al., Astrophys. Space Sci. 309, 365 (2007)

Discussion (2): Association of TASG J1844-038 w/ PSR J1844-0346

PSR J1844-0346

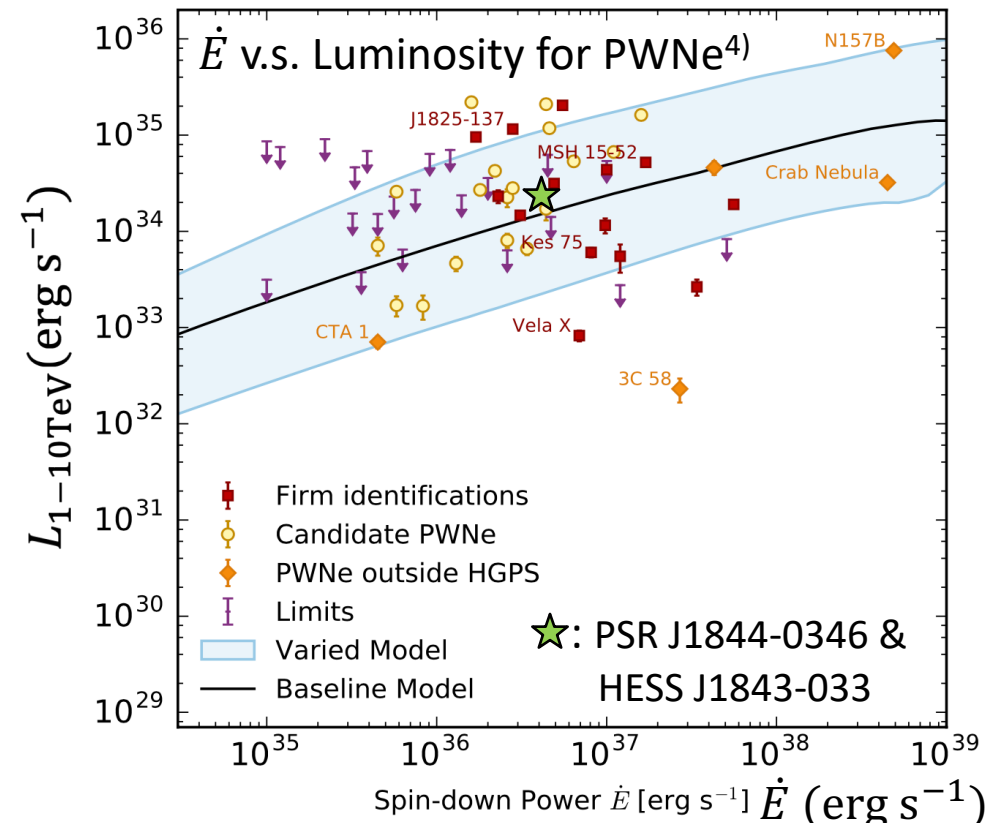
- Gamma-ray PSR discovered by the Einstein@home project¹⁾
- $P = 113 \text{ ms}$, $\tau_c = 12 \text{ kyr}$ & $\dot{E} = 4.2 \times 10^{36} \text{ erg s}^{-1}$
- Pseudo distance: 4.3 kpc²⁾

HESS J1843-033³⁾

- $L(1 \text{ TeV} < E < 10 \text{ TeV}) = 2.4 \times 10^{34} \text{ erg s}^{-1}$ ³⁾ (@ 4.3 kpc)
- Size: $\simeq 18 \text{ pc}$ (@ 4.3 kpc)
- Spectral index: $\simeq 2.0$ (from the ECPL fit in this work)
- => has characteristics typical for **TeV PWNe**⁴⁾.

ICS off CMB is acceptable

- e^\pm w/ $E \approx 90 \text{ TeV}$ scatters off CMB up to $E_{\gamma, \text{cutoff}} \approx 50 \text{ TeV}$ ⁵⁾.
- Size of TASG J1844-038: $\simeq 26 \text{ pc}$ (@ 4.3 kpc)
- Assuming the Geminga-like env.⁶⁾ w/ $B = 3 \mu\text{G}$, $D = 4.4 \times 10^{27} \text{ cm}^2 \text{ s}^{-1}$,
 $\tau_{\text{diff}} \simeq 8 \text{ kyr}$
- Cooling time of e^\pm by sync. & ISC⁵⁾: $\tau_{\text{cool}} \simeq 11 \text{ kyr}$
- => $\tau_{\text{diff}} < \tau_{\text{cool}}$ & $\tau_{\text{diff}} < \tau_c$



- 1) Clark et al., ApJ 834, 106 (2017)
- 2) Devin et al., A&A 647, 68 (2021)
- 3) H.E.S.S. collaboration, A&A 612, A1 (2018)
- 4) H.E.S.S. collaboration, A&A 612, A2 (2018)
- 5) Hinton & Hofmann, Ann. Rev. of Astron. & Astrophys. 47, 523 (2009)
- 6) Abeysekara et al., Science 358, 911 (2017b)

Summary

- Gamma rays from the HESS J1843-033 region observed by the Tibet air shower array
- Detection of TASG J1844-038 above 25 TeV w/ a 6.2σ level
 - Position: $(\alpha, \delta) = (281^\circ 09 \pm 0^\circ 10, -3^\circ 76 \pm 0^\circ 09)$,
consistent w/ HESS J1843-033, eHWC J1842-035, & LHAASO J1843-0338.
 - Extension: $0.34^\circ \pm 0.12^\circ$
- Energy spectrum measured in $25 \text{ TeV} < E < 130 \text{ TeV}$ for the 1st time
 - Our results is fitted w/ $dN/dE = (9.70 \pm 1.89) \times 10^{-16} (E/40 \text{ TeV})^{-3.26 \pm 0.30} \text{ TeV}^{-1} \text{ cm}^{-2} \text{ s}^{-1}$.
 - Combined spectra b/w HESS, LHAASO & TASG implies a cutoff @ $49.5 \pm 9.0 \text{ TeV}$.
- Source association w/ nearby objects
 - If SNR G28.6-0.1 is assumed to be the source, possibly π^0 -decay gamma rays from CR protons w/
 $E \lesssim 500 \text{ TeV}$ contribute to the total emission and the SNR could have been a PeVatron in the past.
 - If PSR J1844-0346 is assumed to be, the emission can be well explained by ICS off CMB by electrons
w/ $E \lesssim 90 \text{ TeV}$ accelerated by a TeV PWN.

Thank you

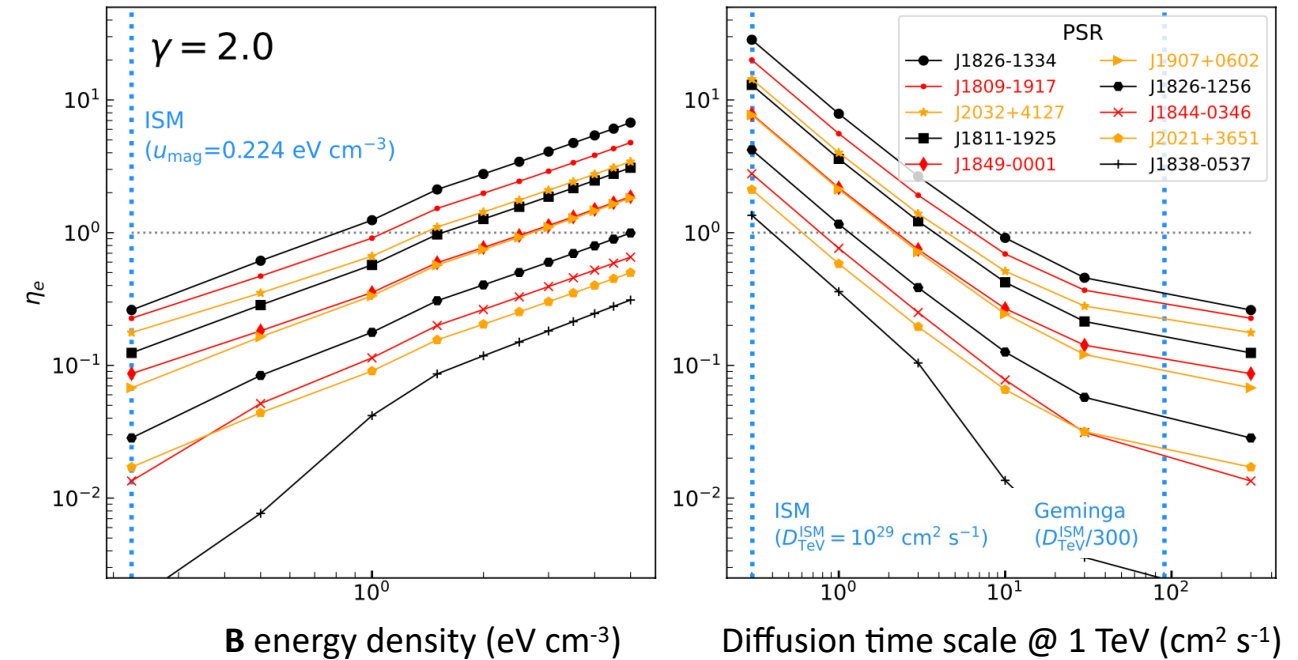
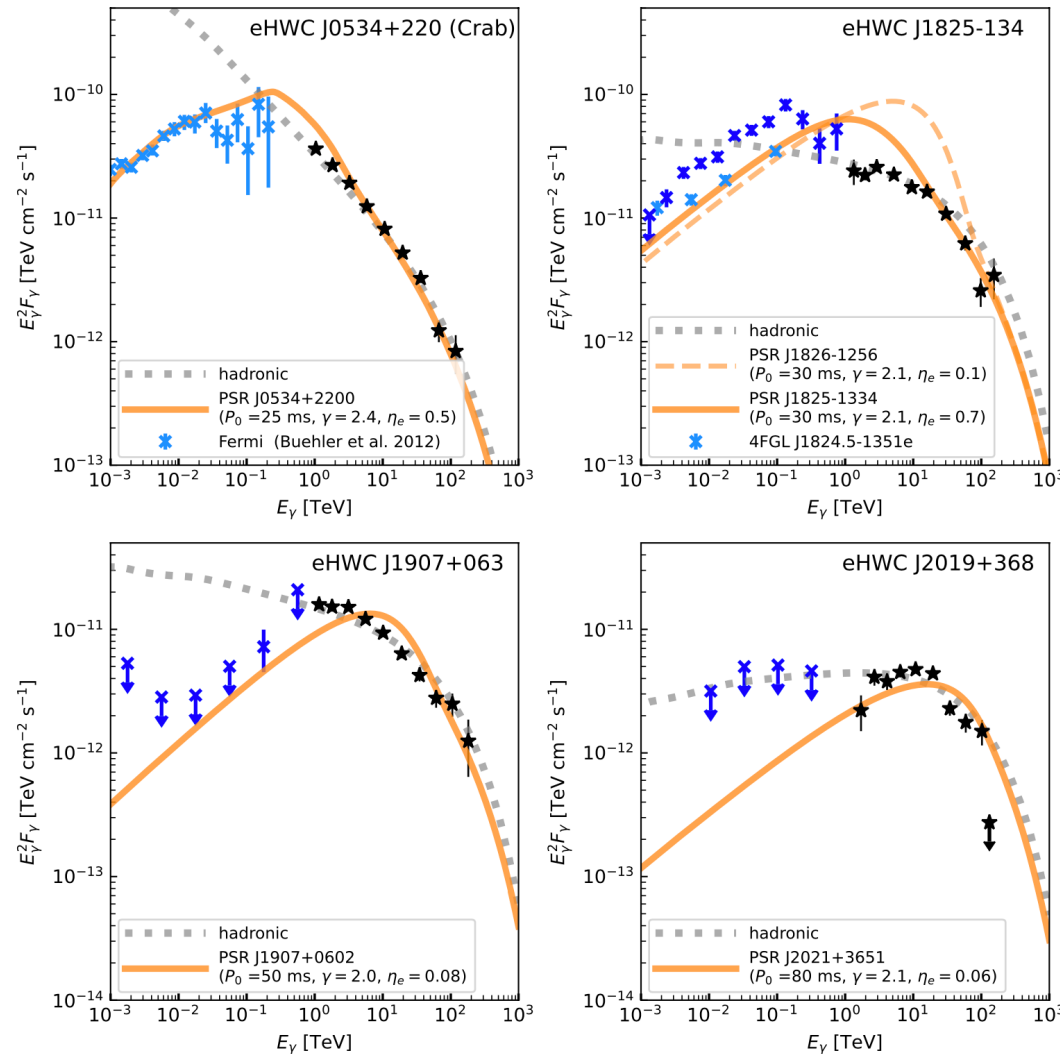
Feel free to ask a question or send me an email to
katosei@icrr.u-tokyo.ac.jp

If you are interested in my presentation, please also read
“*Measurement of the Gamma-Ray Energy Spectrum beyond 100 TeV from the HESS J1843-033 Region*”,
Amenomori et al., ApJ 932, 120 (2022)
(<https://doi.org/10.3847/1538-4357/ac6ef4>)

Back-up slides

Theoretical research (1)

Sudoh et al. (2021): All eHWC sources are TeV PWN or TeV halo powered by nearby pulsars



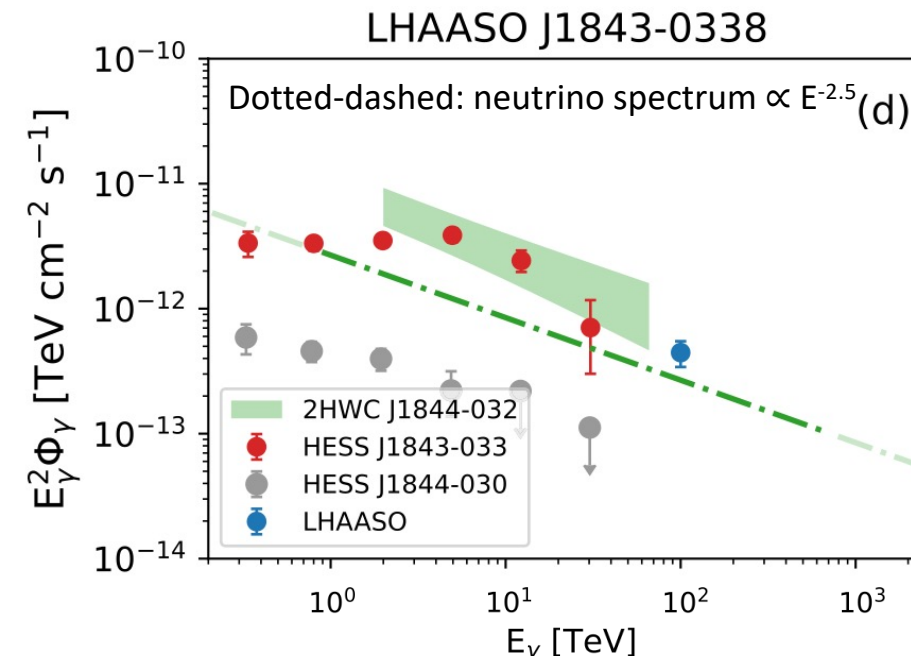
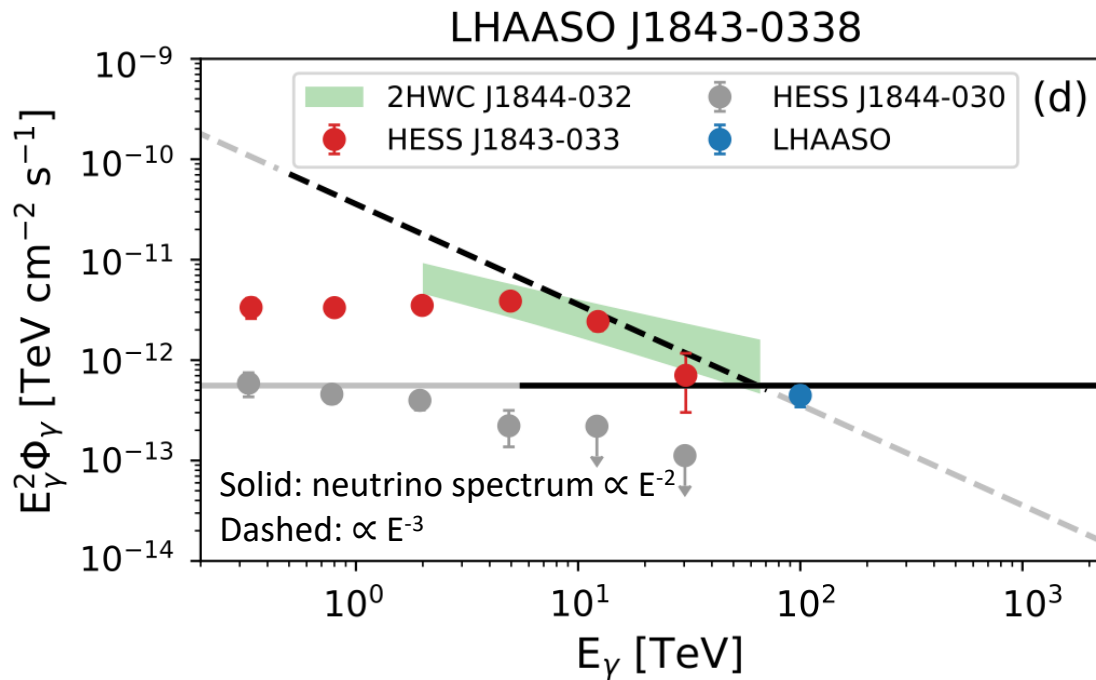
Fit result for HESS J1843-033 is not shown in their paper

Theoretical research (2)

Huang & Li (2022): Ratio of hadronic gamma-ray flux to the total flux using the observation results of neutrinos

$$\Phi_{\gamma}^{\text{UL}}(100 \text{ TeV}) = \frac{1}{2} \Phi_{\nu_{\mu} + \bar{\nu}_{\mu}}^{\text{UL}}(E_{\nu}) \left(\frac{50 \text{ TeV}}{E_{\nu}} \right)^{-\gamma},$$

90% upper limit on hadronic gamma-ray flux

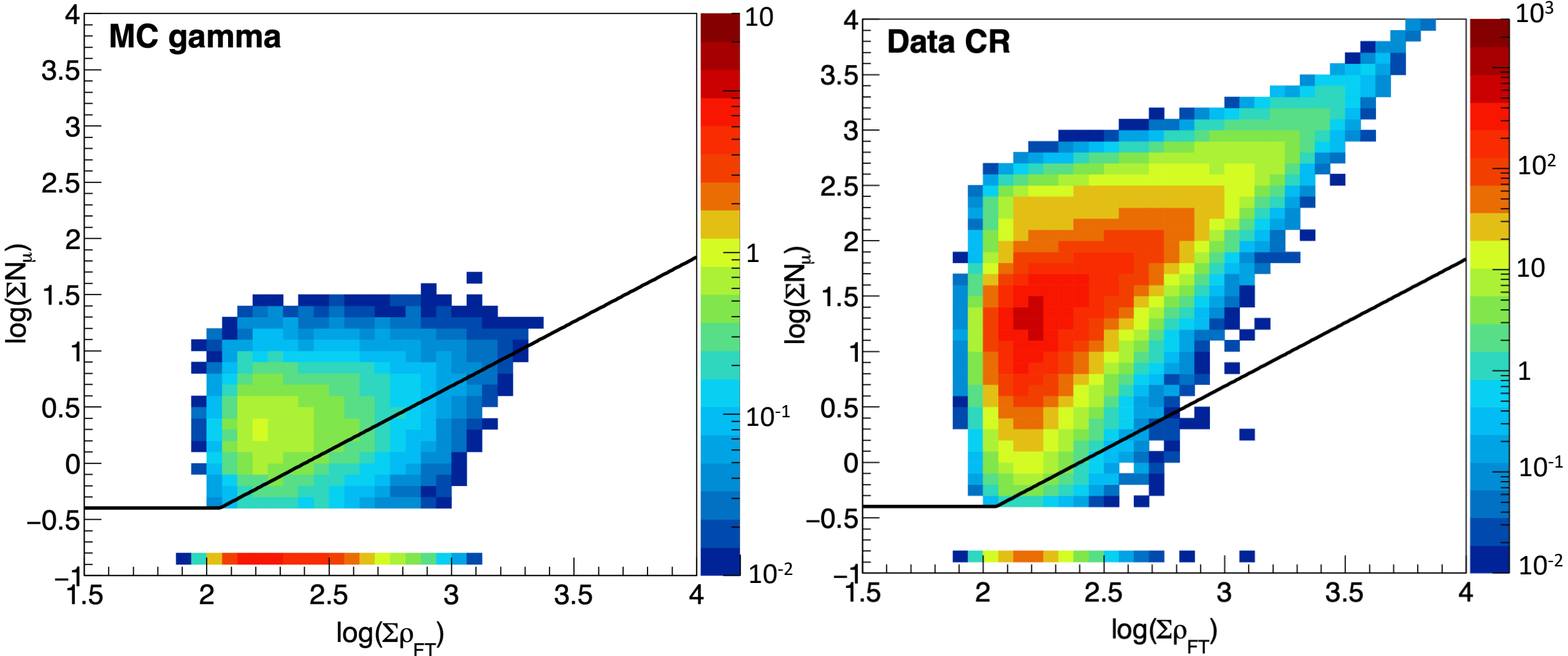


- In these theoretical works (Sudoh et al and Huang & Li), association between gamma-ray sources remains unclear (not evaluated clearly) because energy spectrum in $30 \text{ TeV} < E < 100 \text{ TeV}$ is not measured systematically
- Discussion by experimentalists is not enough (only vague deduction for the association is made)

Data analysis for gamma rays from the HESS J1843-033 region

- Used data: 2014 Feb. to 2017 May (719 live days)
- Event selection criteria: the same as the Crab std. cut (Amenomori et al., PRL 123, 051101, 2019)
EXCEPT for the following two points:
 1. **zenith < 50 deg** to improve statistics ($\text{zenith}_{\text{meridian}} = 33 \text{ deg}$), and
 2. Optimized MD cut: $\Sigma N\mu < 1.8 \times 10^{-3} (\Sigma \rho/m^2)^{1.1}$ or $\Sigma N\mu < 0.4$.
($\Sigma \rho$: Sum of # density recorded by each detectors of the AS array)
- # of events after the selection: 1.4×10^7 events

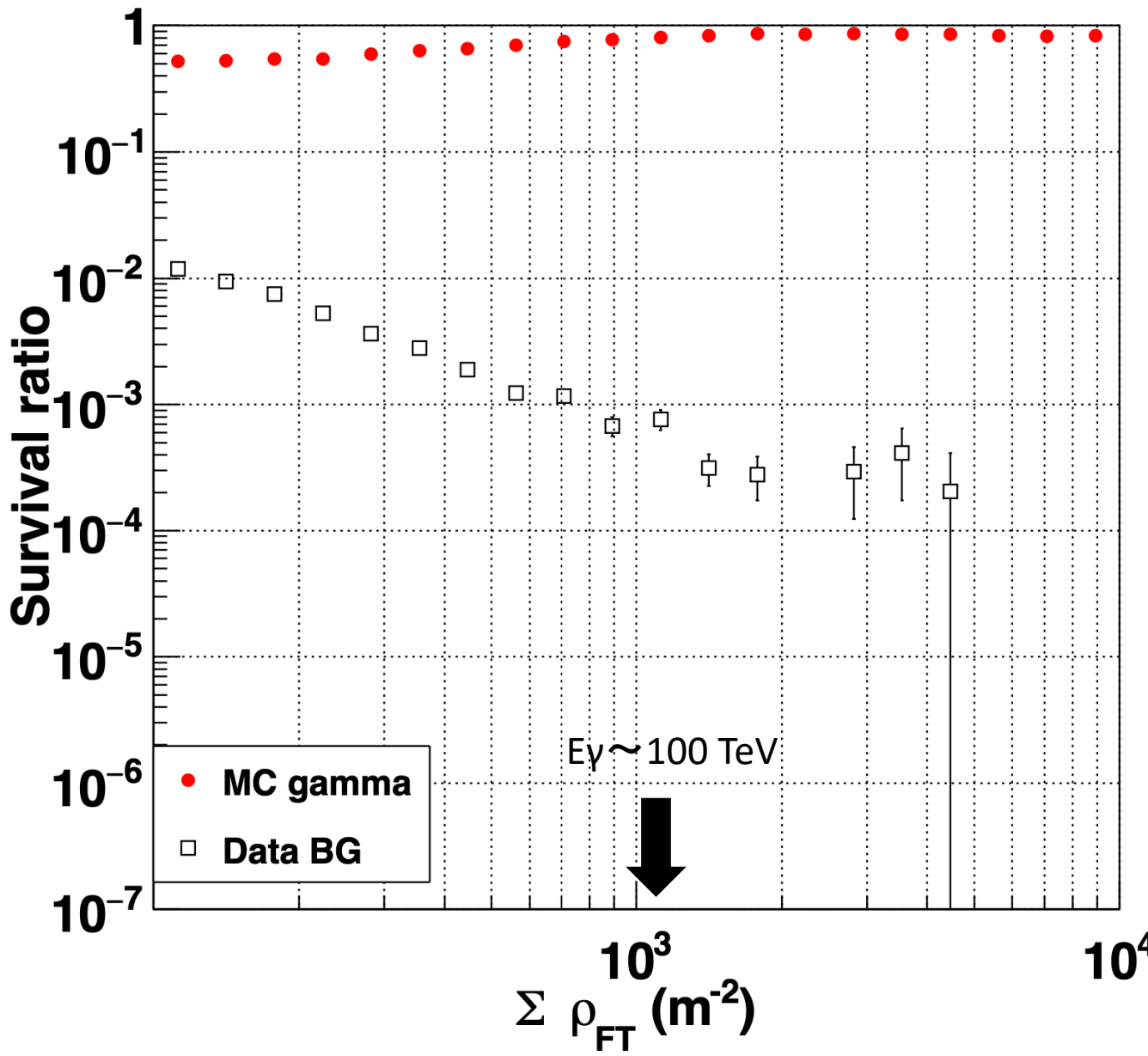
Optimum MD cut line (1): Cut-line formula



$$\Sigma N_\mu < 1.8 \times 10^{-3} (\Sigma \rho / m^{-2})^{1.1} \text{ or } \Sigma N_\mu < 0.4$$

Optimum MD cut line (2): Survival ratio of gamma rays & BGCRs

Gamma & BG survival ratio



@ $E\gamma \sim 100 \text{ TeV}$

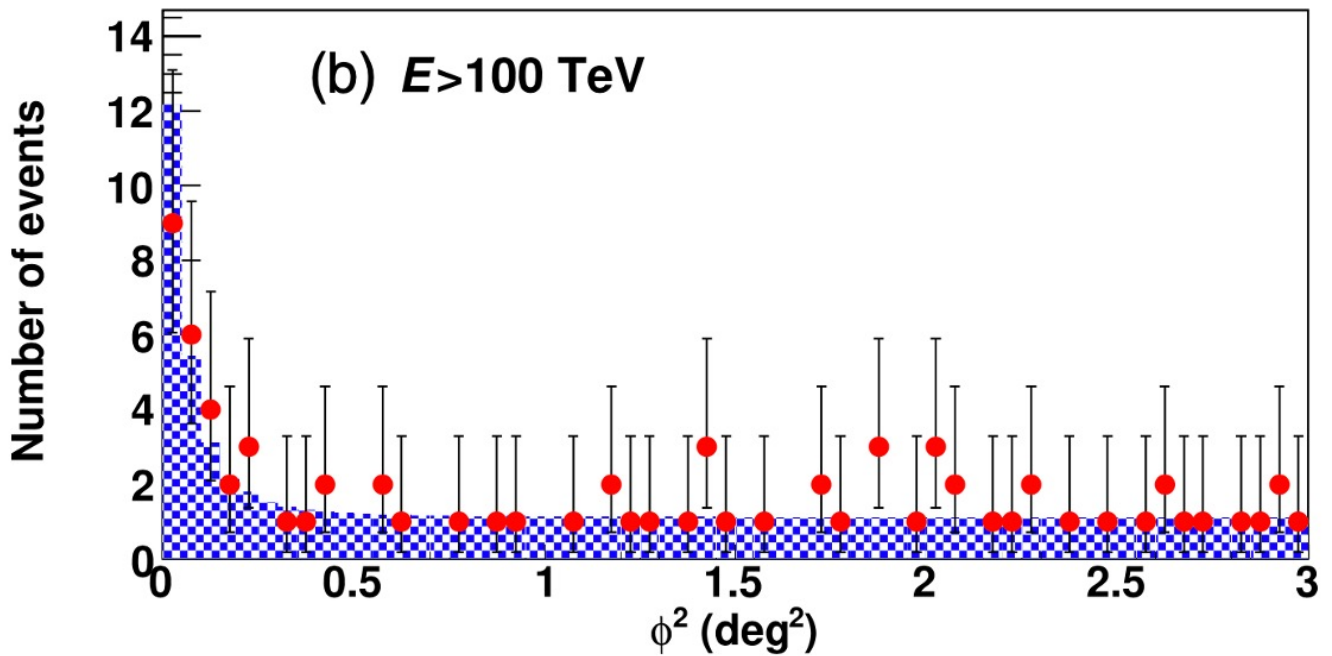
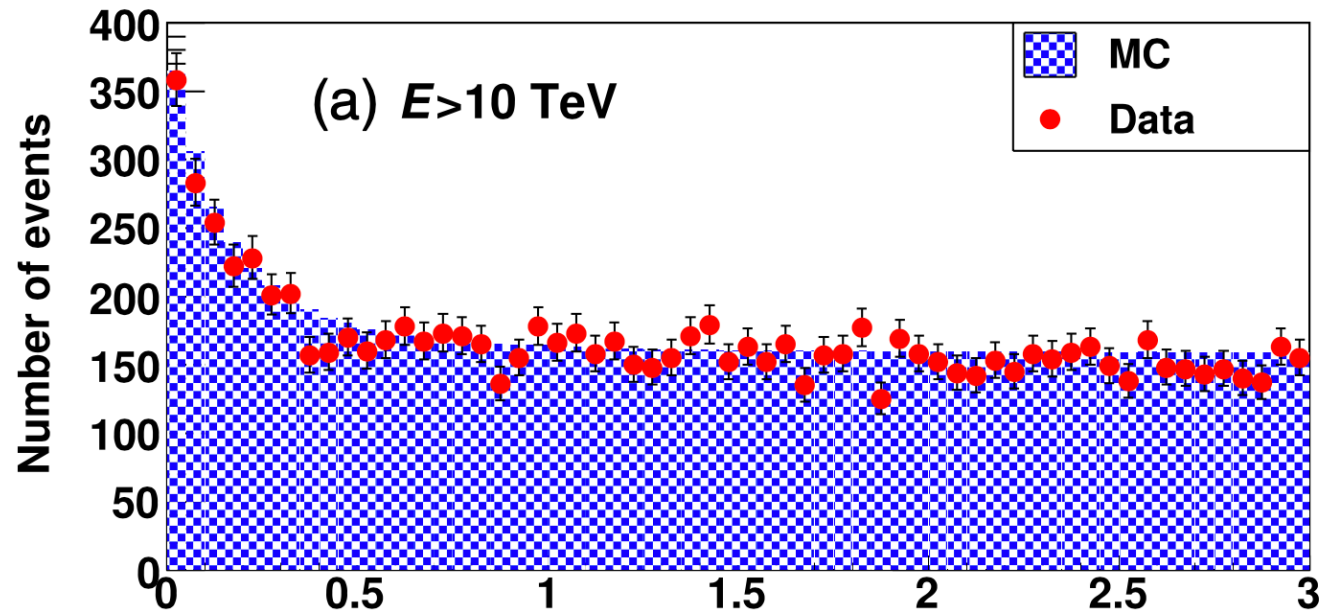
Gamma survival ratio: $\simeq 81\%$

BG rejection power: $\gtrsim 99.9\%$

Point spread function

ϕ^2 distribution for the Crab Nebula

(Amenomori et al., PRL 123, 051101, 2019)



Estimation of positional uncertainty of a gamma-ray source

- For TASG J1844-038, eHWC J1842-035, & LHAASO J1843-0338 :
Positional uncertainty is evaluated in terms of the error radius $R_{0.68}$ w/ the 68% C.L.
as in *HESS collaboration, A&A 612, A1 (2018)*, but using uncertainties of α & δ instead of l & b ;

$$R_{0.68} = f_{0.68} \sqrt{\Delta\alpha_{\text{stat}}^2 + \Delta\alpha_{\text{sys}}^2 + \Delta\delta_{\text{stat}}^2 + \Delta\delta_{\text{sys}}^2}$$

where $f_{0.68} = \sqrt{-2 \ln(1 - 0.68)}$ (A. A. Abdo et al. ApJS, 183, 46, 2009b) and

$\Delta\alpha_{\text{stat (sys)}}$ & $\Delta\delta_{\text{stat (sys)}}$ are the statistical (systematic) uncertainties of α & δ , respectively.

- HESS sources :
There $R_{0.68}$'s are cited from *HESS collaboration, A&A 612, A1 (2018)*:

Relation of the TASG position to nearby gamma-ray sources

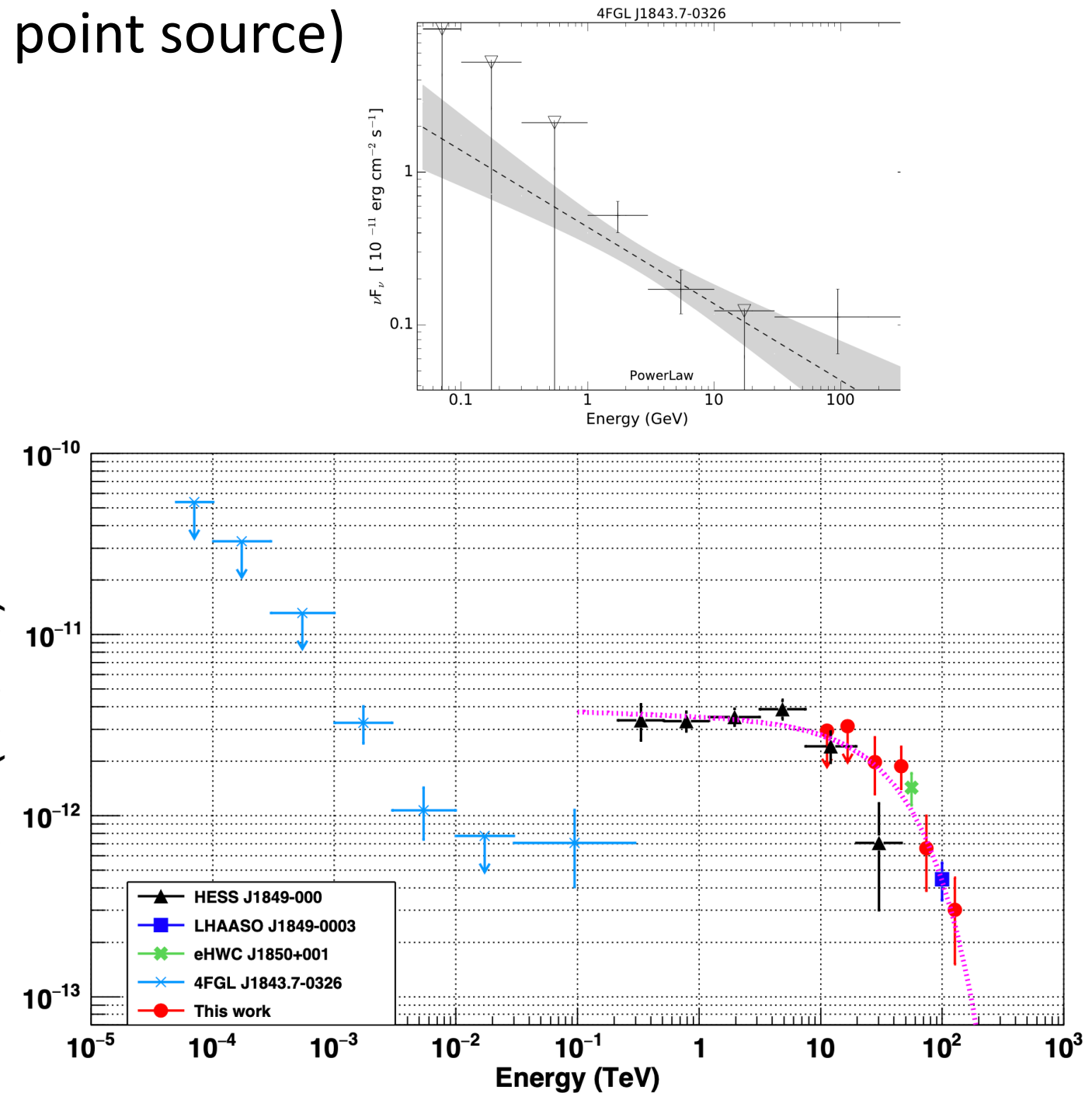
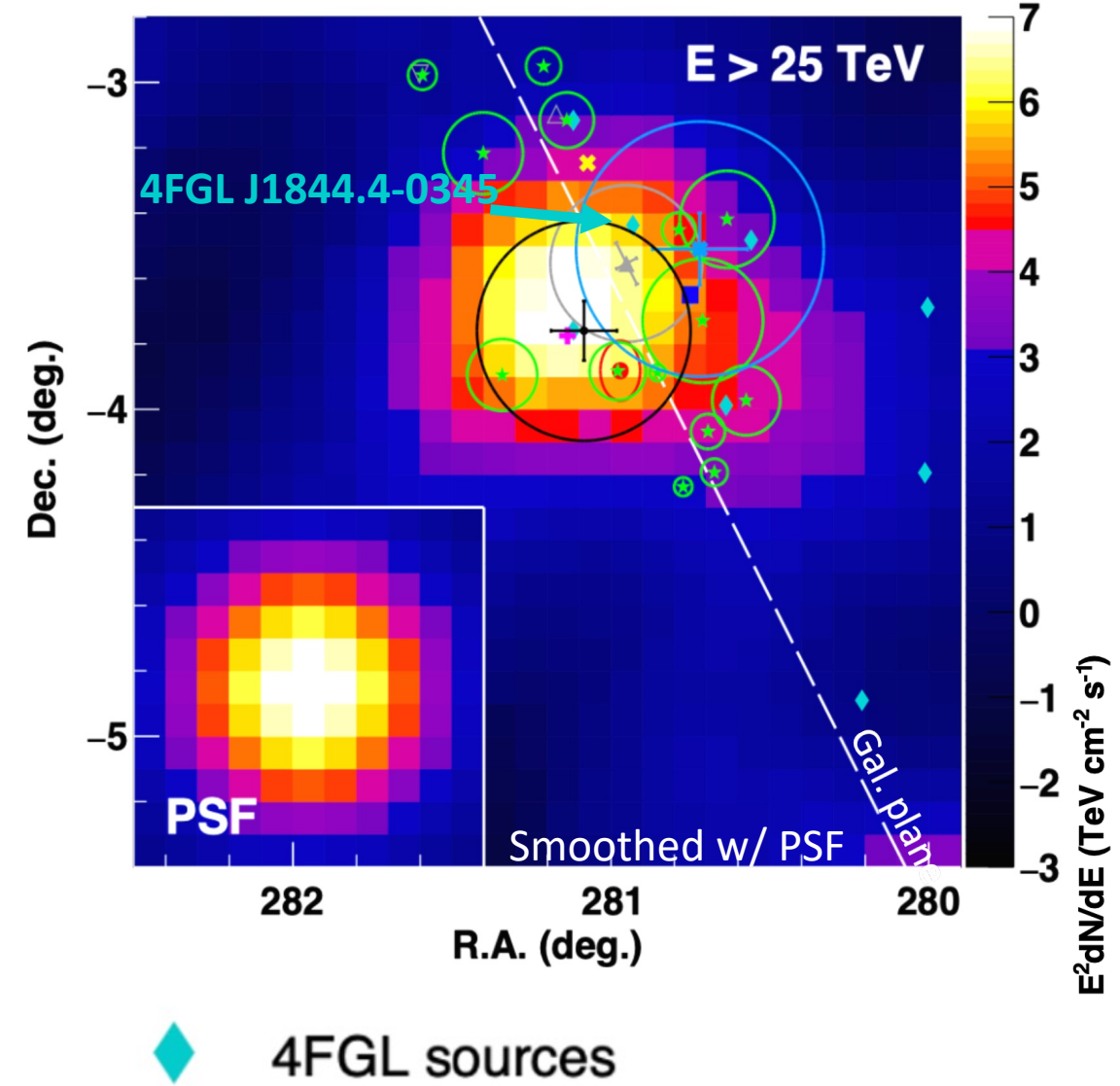
Source name	$\alpha(^{\circ})$	$\delta(^{\circ})$	$R_{0.68}^{\dagger}(^{\circ})$	Extension ($^{\circ}$)	Angular distance to TASG J1844-038 ($^{\circ}$)
TASG J1844-038	281.09	-3.76	0.21	0.35 ± 0.11	-
HESS J1843-033	280.95	-3.55	0.12	0.24 ± 0.06	0.25 (1.0σ)
HESS J1844-030	281.17	-3.10	0.023	0.02 ± 0.013	0.67 (3.2σ)
HESS J1846-029	281.60	-2.97	0.015	0.01 ± 0.013	0.94 (4.5σ)
eHWC J1842-035	280.72	-3.51	0.30	0.39 ± 0.09	0.44 (1.2σ)
LHAASO J1843-0338	280.75	-3.65	0.16	-*	0.35 (1.4σ)

[†] For $R_{0.68}$, see HESS collaboration, A&A 612, A1 (2018)

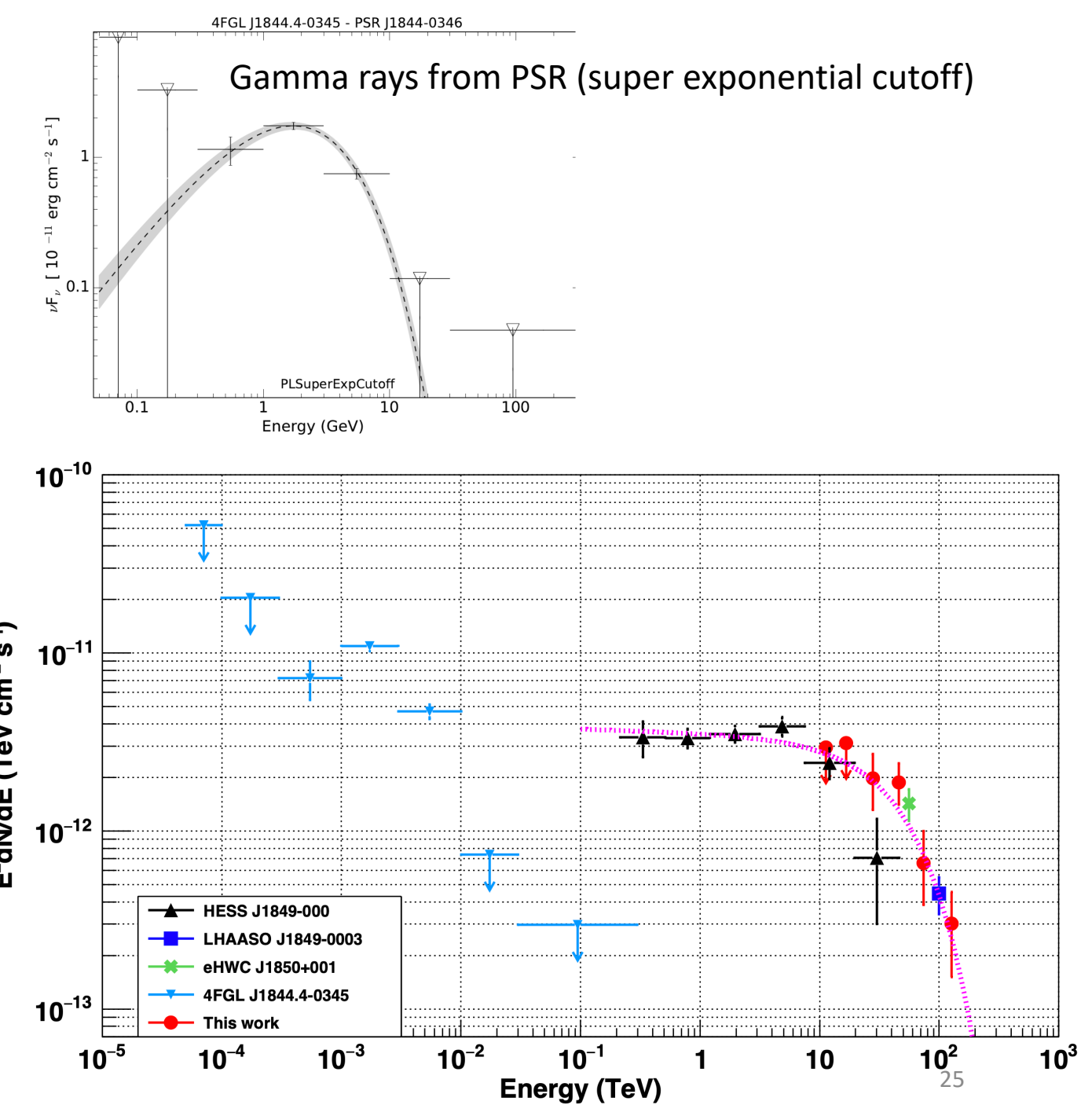
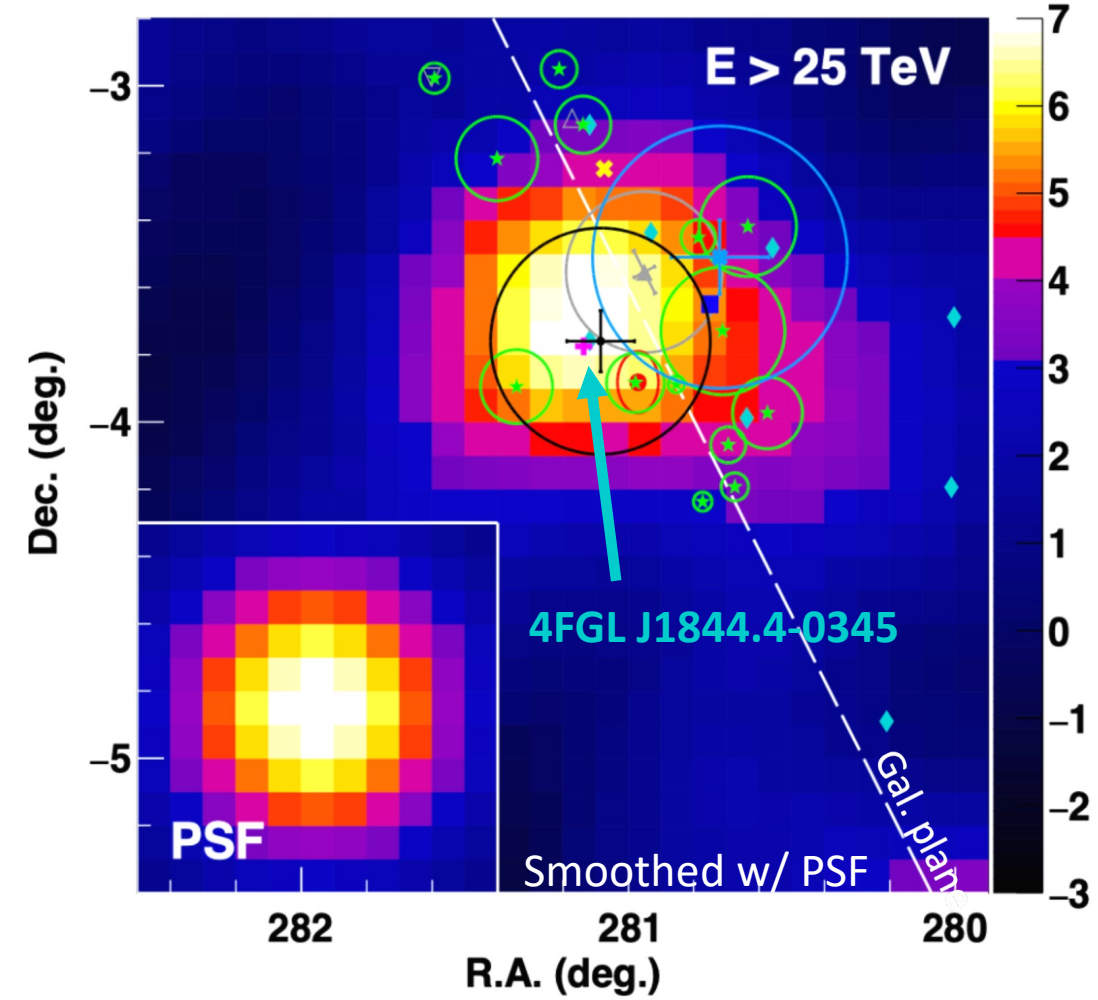
* The source extension is not published

- The position of TASG J1844-038 is
 - consistent w/ those of HESS J1843-033, eHWC J1842-035, and LHAASO J1843-0338, but
 - deviated from HESS J1844-030 and HESS J1846-029.

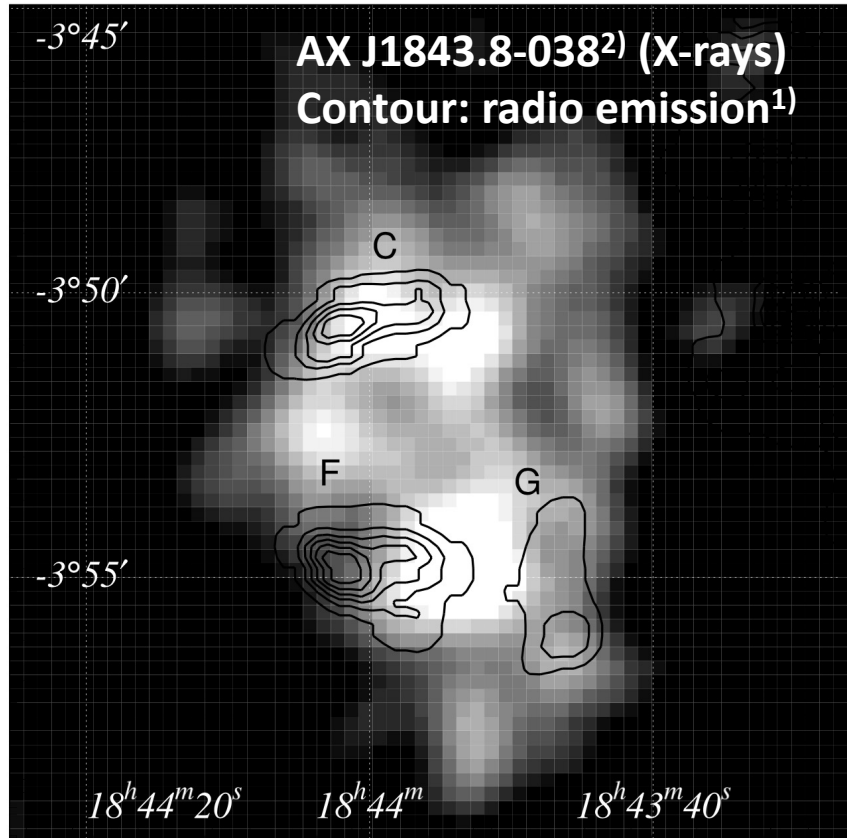
4FGL J1843.7-0326 (cataloged as a point source)



4FGL J1844.4-0345



Multi-wavelength flux (radio & X-ray bands) (1): The SNR G28.6-0.1 region



(a) Radio flux^{2, 3)} @ 6 cm: 0.9 Jy
21 cm: 2.1 Jy

(b) X-ray observation⁴⁾

TABLE 1
BEST-FIT MODEL PARAMETERS FOR AX J1843.8–0352

PARAMETER	POWER LAW			NEI Observation 1+2
	Observation 1	Observation 2	Observation 1+2	
Photon index.....	$2.4^{+1.1}_{-0.9}$	$2.1^{+0.4}_{-0.4}$	$2.1^{+0.4}_{-0.3}$...
kT (keV).....	$5.4^{+3.5}_{-1.6}$
Abundance ^a	$0.17^{+0.17}_{-0.14}$
$\log [n_e t]$ ($\text{cm}^{-3} \text{s}$).....	$11.1^{+0.4}_{-0.7}$
N_{H} (10^{22} cm^{-2}).....	$4.7^{+2.8}_{-1.8}$	$3.7^{+0.7}_{-0.6}$	$3.8^{+0.7}_{-0.6}$	$3.5^{+0.6}_{-0.5}$
Absorbed flux ^b ($10^{-14} \text{ ergs cm}^{-2} \text{s}^{-1} \text{arcmin}^{-2}$).....	2.3	3.1	3.1 ^c	3.0 ^c
Unabsorbed flux ^d ($10^{-14} \text{ ergs cm}^{-2} \text{s}^{-1} \text{arcmin}^{-2}$)....	3.6	4.3	4.3 ^c	4.1 ^c
χ^2/dof	18.9/27	48.1/52	68.1/81	65.3/79

NOTE.—The errors correspond to 90% confidence.

^a Assuming the solar abundance ratio (Anders & Grevesse 1989).

^b Observed flux per unit area (arcmin^2) in the energy band 2.0–10.0 keV.

^c The fluxes of observations 1+2 are calculated from the normalizations for the spectrum of observation 2, which covers the whole of AX J1843.8–0352.

^d Absorption-corrected flux per unit area (arcmin^2) in the energy band 2.0–10.0 keV.

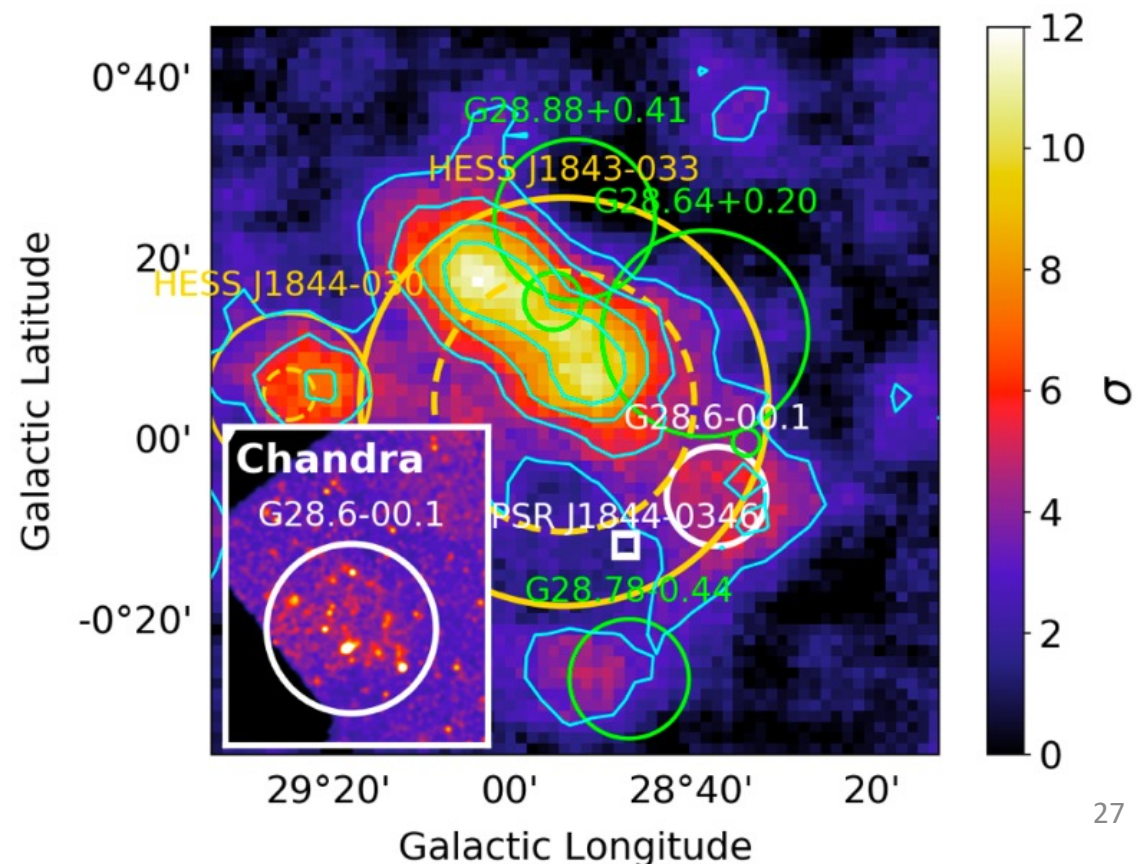
- 1) Bamba et al., PASJ 53, L21 (2001)
- 2) Altenhoff et al., A&AS 35, 23 (1979)
- 3) Helfand et al., ApJ 341, 151 (1989)
- 4) Ueno et al., ApJ 588, 338 (2003)

Multi-wavelength flux (radio & X-ray bands) (1): The PSR J1844-0346 region

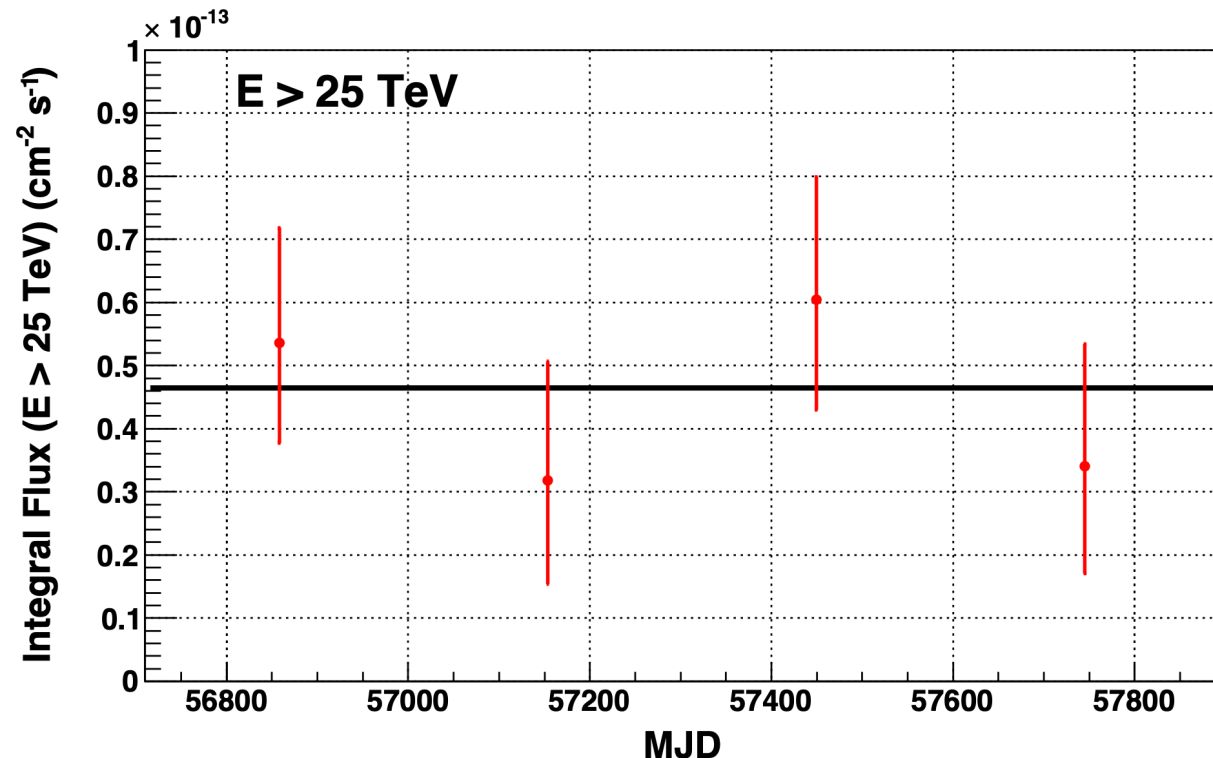
According to Devin et al., A&A 647, A68 (2021),

We also explored the archival multiwavelength data toward the pulsar PSR J1844–0346 and we did not find any radio or X-ray counterpart that could indicate a possible PWN. Radio data from MAGPIS and infrared data from *Spitzer* show a bright extended emission southeast of PSR J1844–0346. . .

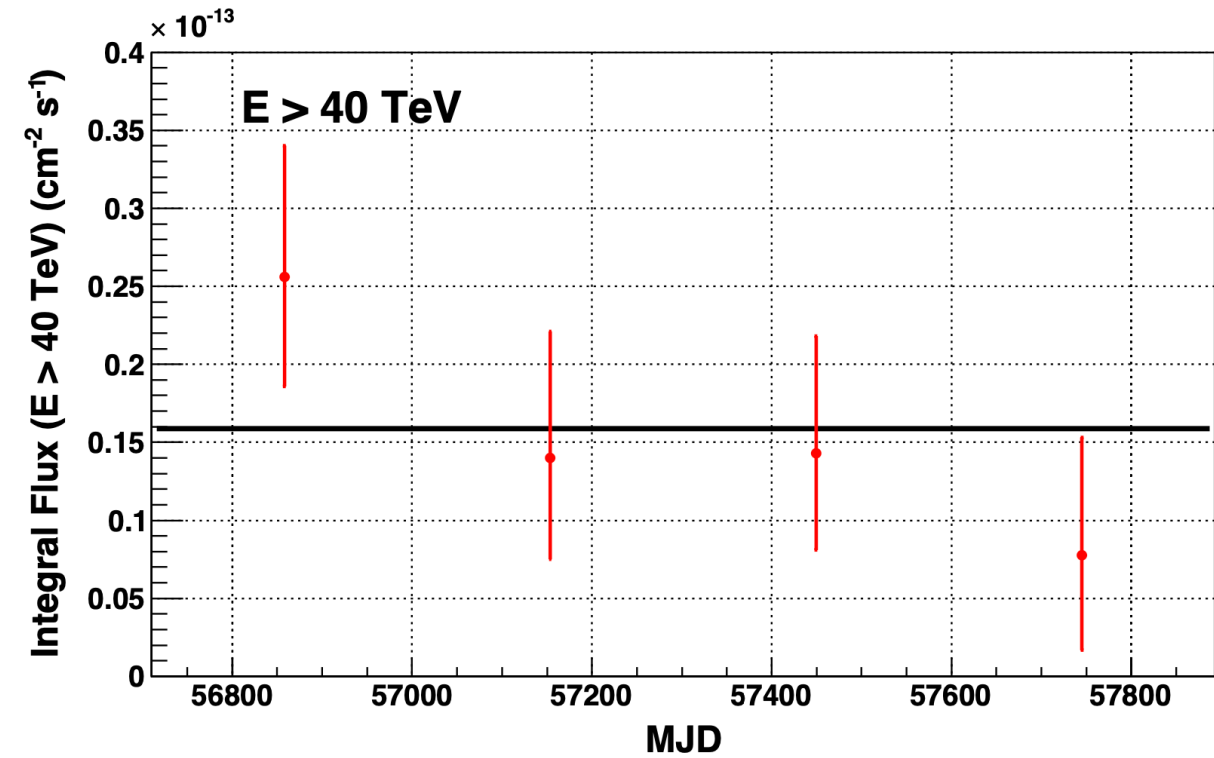
Significance map of gamma-ray emission → observed by HESS (Devin et al., 2021)



Results (4): Time variation of the integral flux



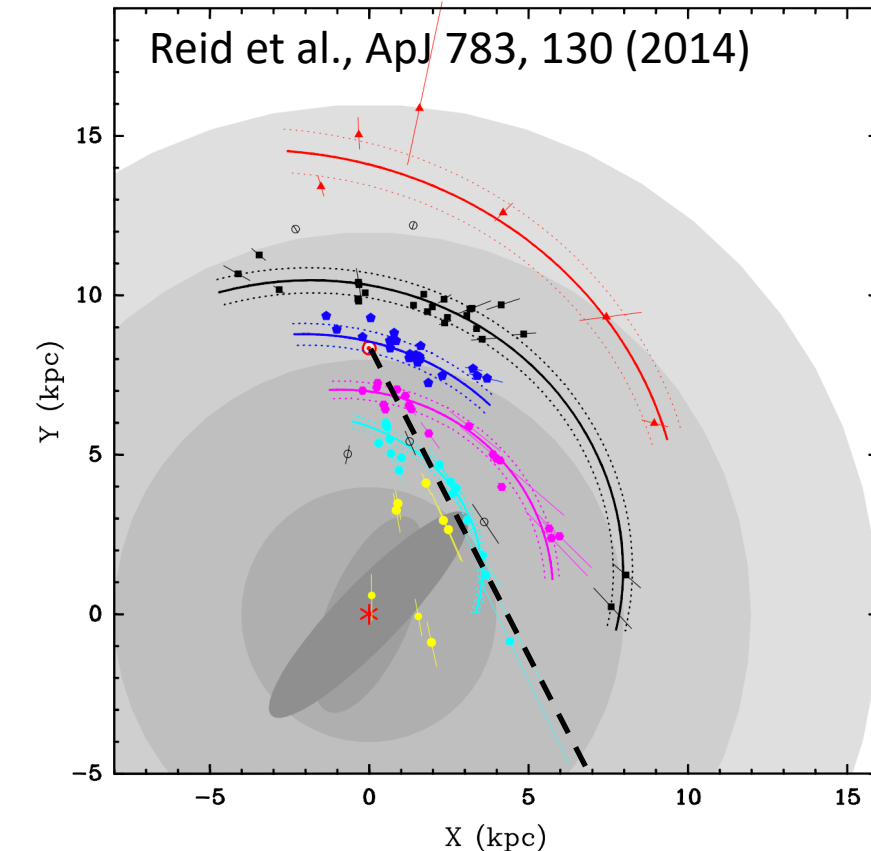
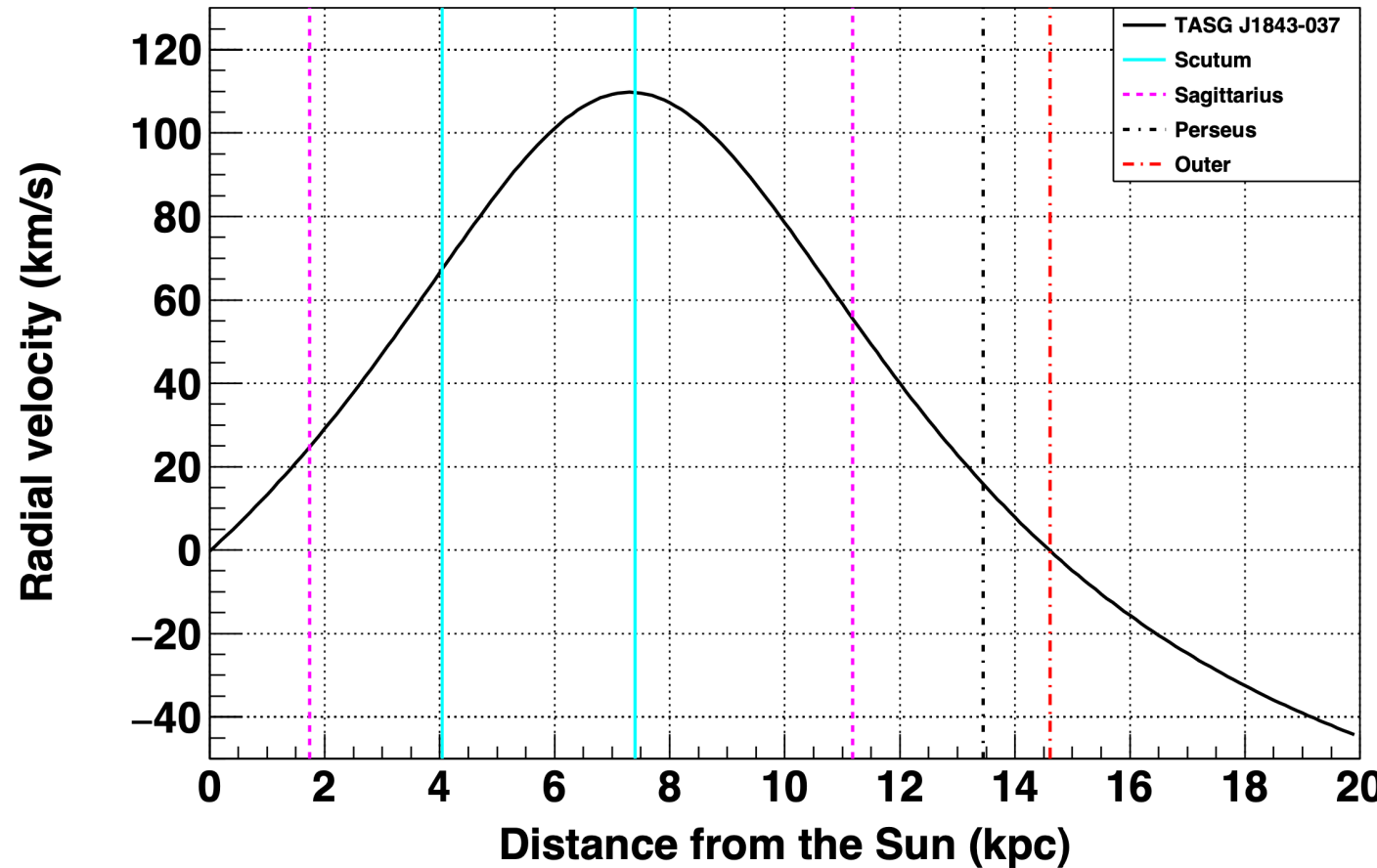
Consistent w/ stable @ $(4.65 \pm 0.89) \times 10^{-14} \text{ cm}^{-2} \text{s}^{-1}$
 $(\chi^2 = 1.9/3)$



Consistent w/ stable @ $(1.59 \pm 0.38) \times 10^{-14} \text{ cm}^{-2} \text{s}^{-1}$
 $(\chi^2 = 3.2/3)$

No variation of the flux by $\sim 30\%$ in $\lesssim 1$ yr time scale is found

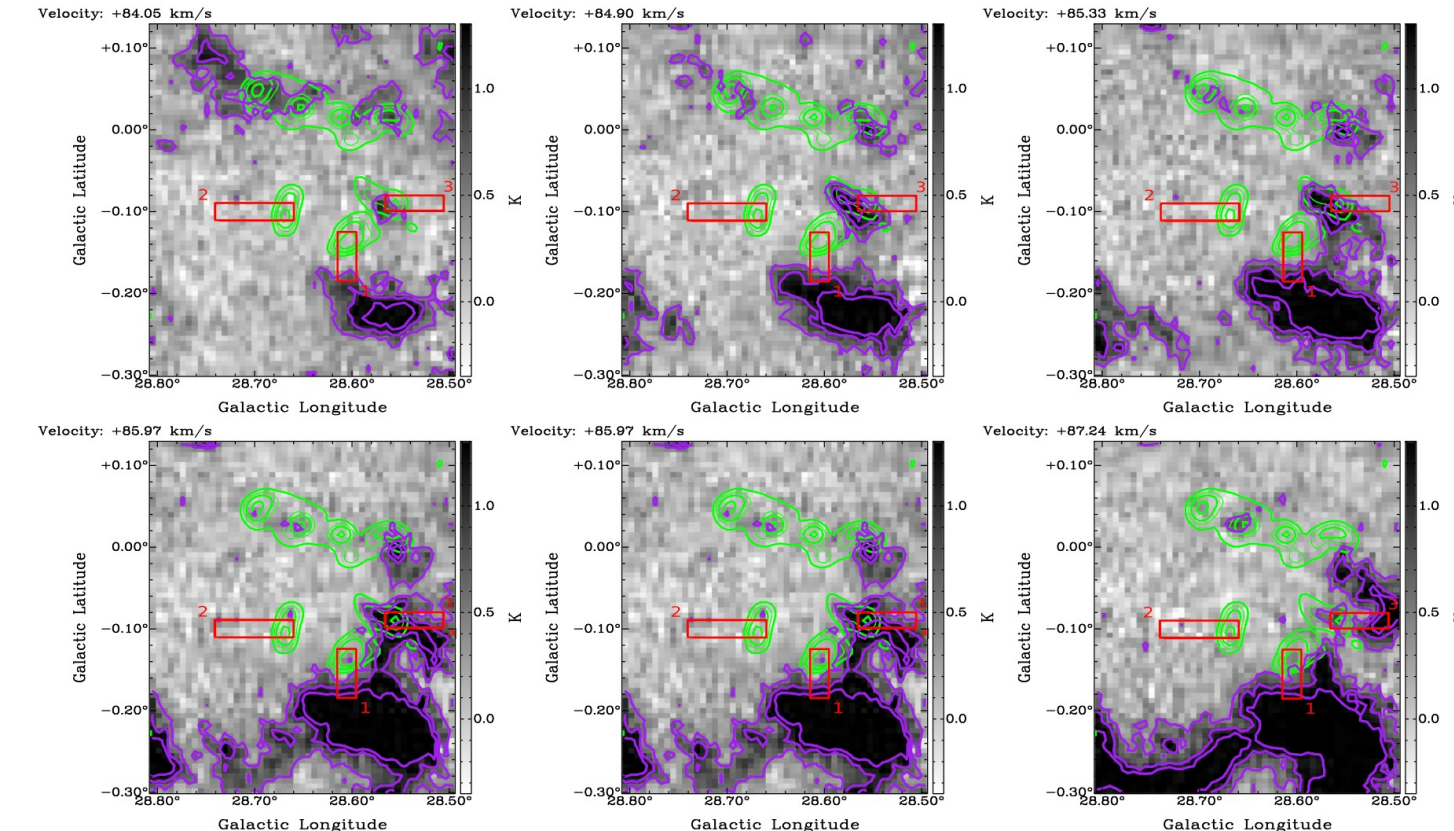
Distance-Vrad relation in the direction of TASG J1844-038 ($I = 28.8$ deg)



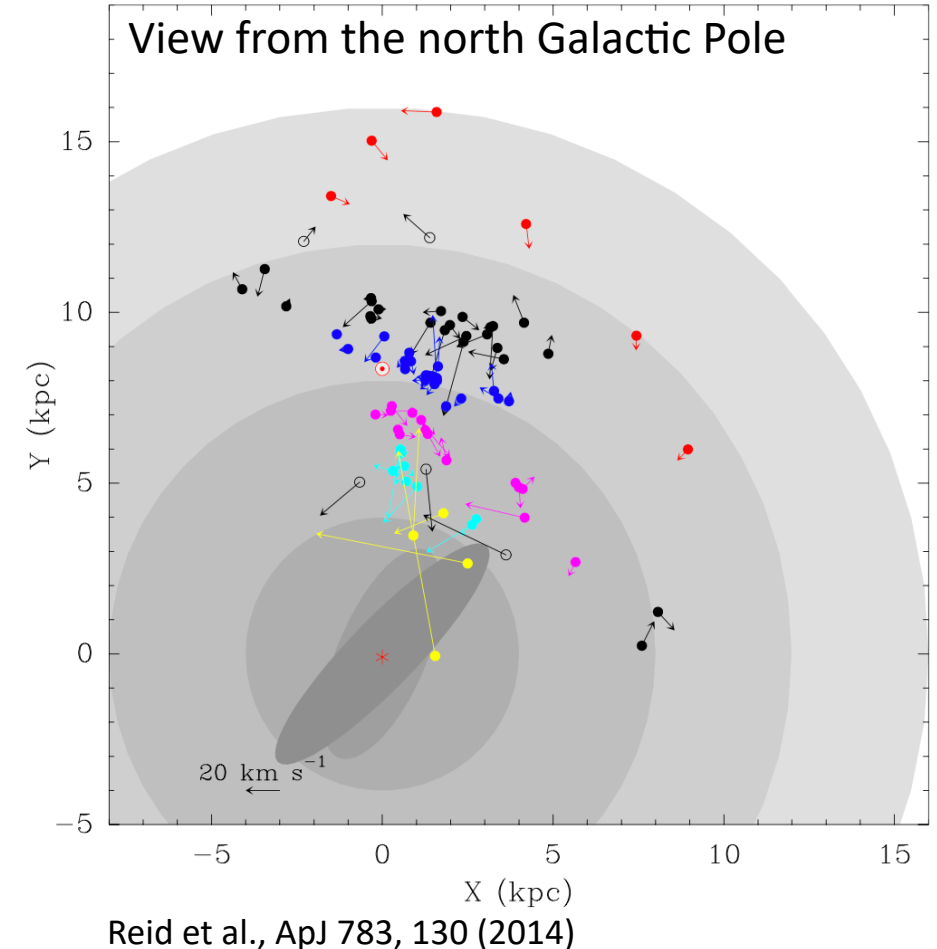
$$\ln(R/R_{\text{ref}}) = -(\beta - \beta_{\text{ref}}) \tan \psi$$

Arm	N	β_{ref} (β Range) (deg)	R_{ref} (kpc)	Width (kpc)	ψ (deg)
Scutum	17	27.6 (+3 → 101)	5.0 ± 0.1	0.17 ± 0.02	19.8 ± 2.6
Sagittarius	18	25.6 (-2 → 68)	6.6 ± 0.1	0.26 ± 0.02	6.9 ± 1.6
Local	25	8.9 (-8 → 27)	8.4 ± 0.1	0.33 ± 0.01	12.8 ± 2.7
Perseus	24	14.2 (-21 → 88)	9.9 ± 0.1	0.38 ± 0.01	9.4 ± 1.4
Outer	6	18.6 (-6 → 56)	13.0 ± 0.3	0.63 ± 0.18	13.8 ± 3.3

Interval of the integration over the velocity range



Ranasinghe & Leahy, MNRAS 477, 2243 (2018)

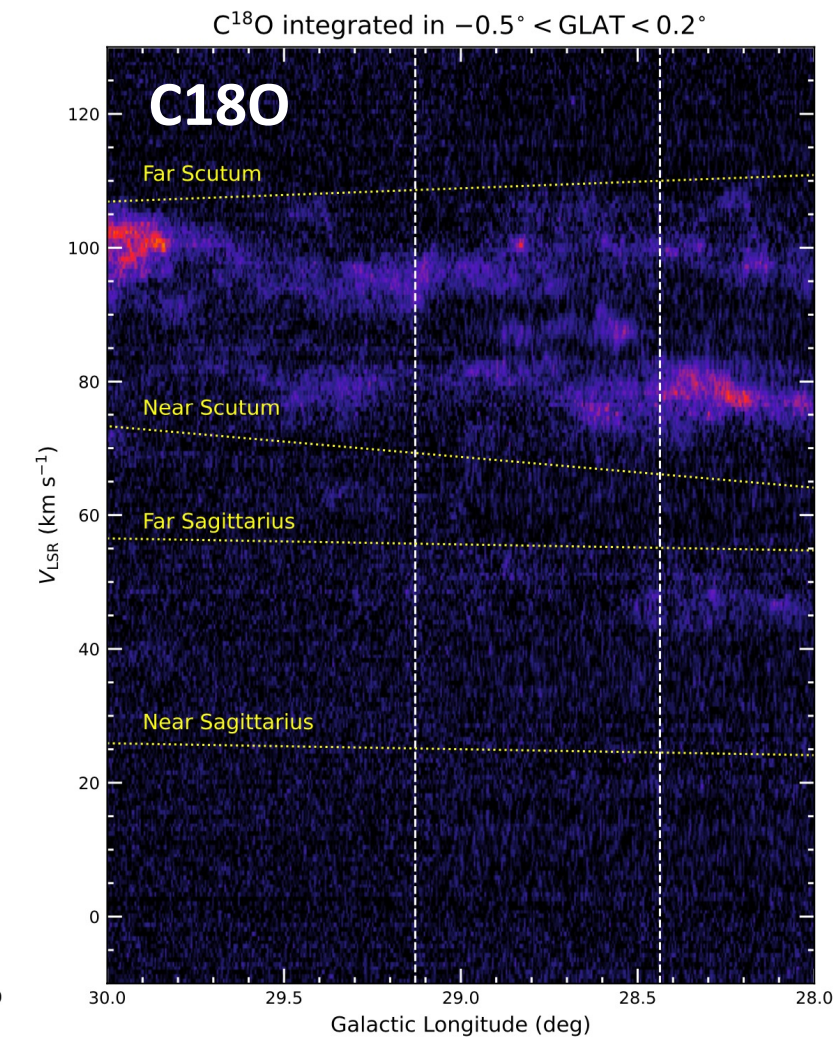
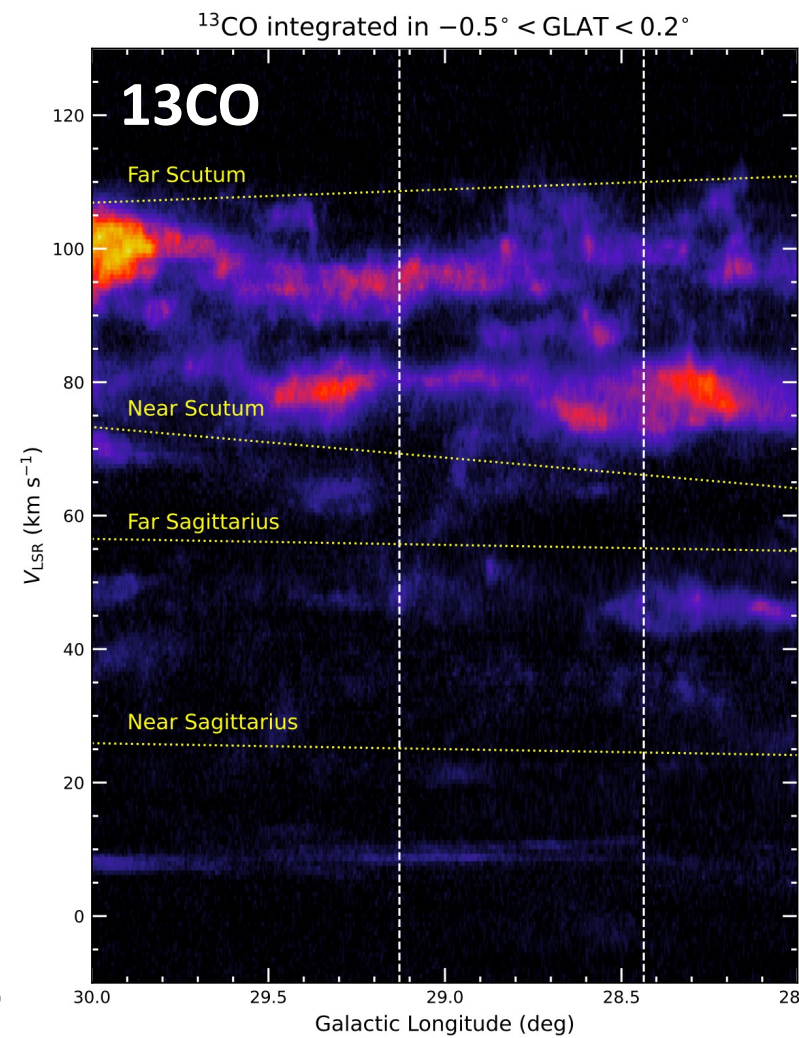
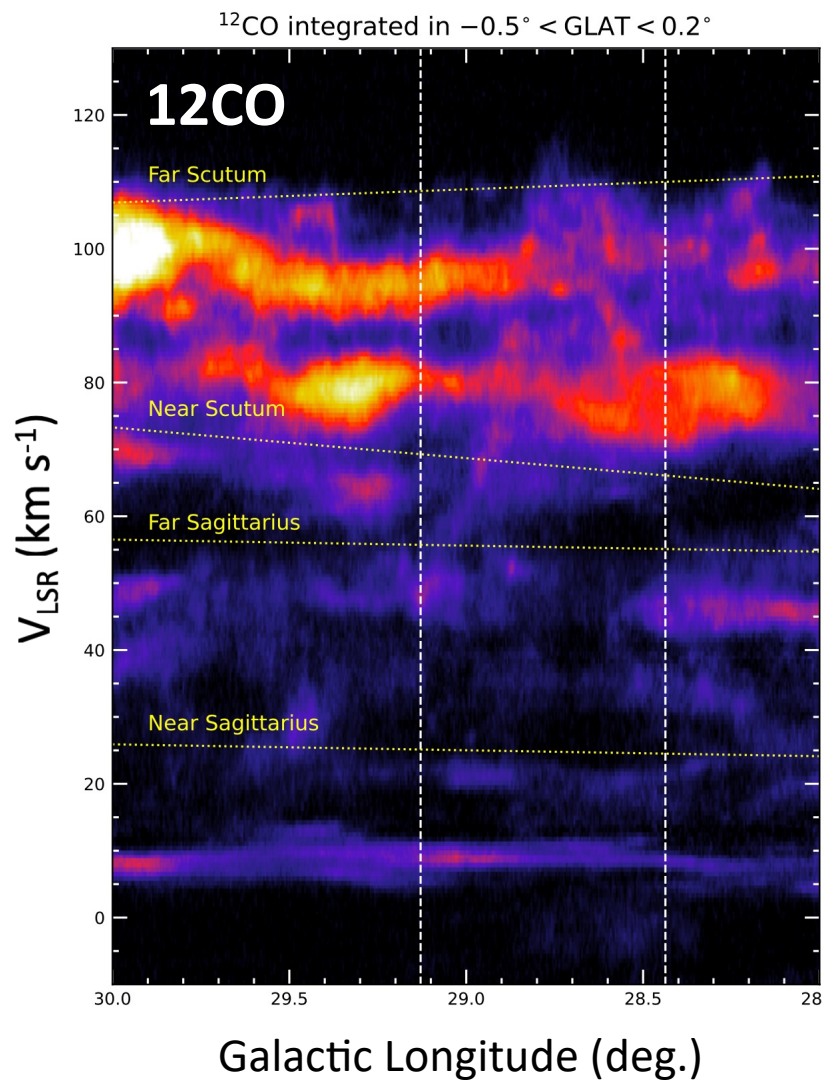


Reid et al., ApJ 783, 130 (2014)

- SNR G28.6-0.1 are interacting w/ molecular clouds in the $v \simeq 85$ km/s channels (left)
- On the other hand, generally celestial objects in the Galaxy have their **peculiar motion w/ ~ 20 km/s** (right)
- We determine the interval of integration over **the velocity range of 20 km/s centered at 85 km/s**

Comparison b/w ^{12}CO , ^{13}CO and C^{18}O

Galactic longitude v.s. V_{LSR}



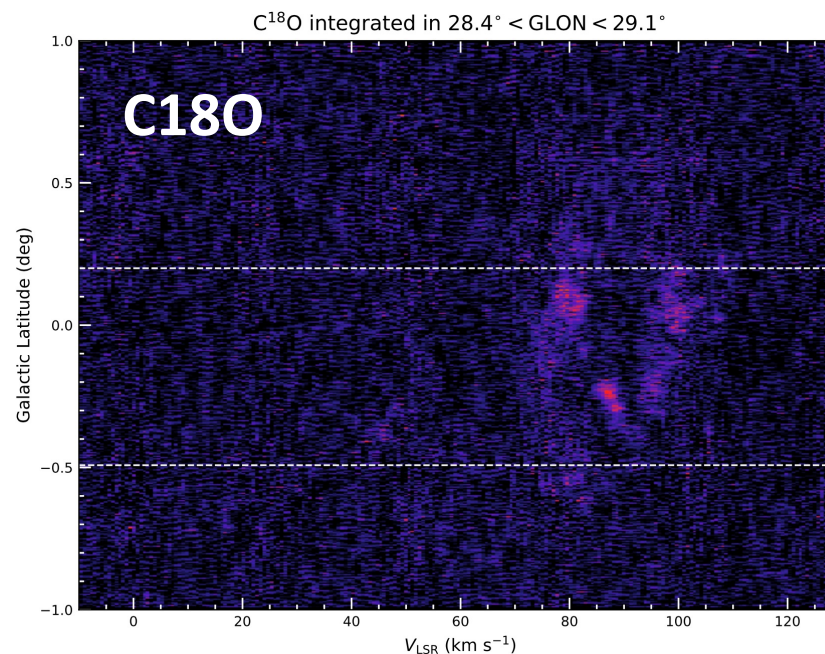
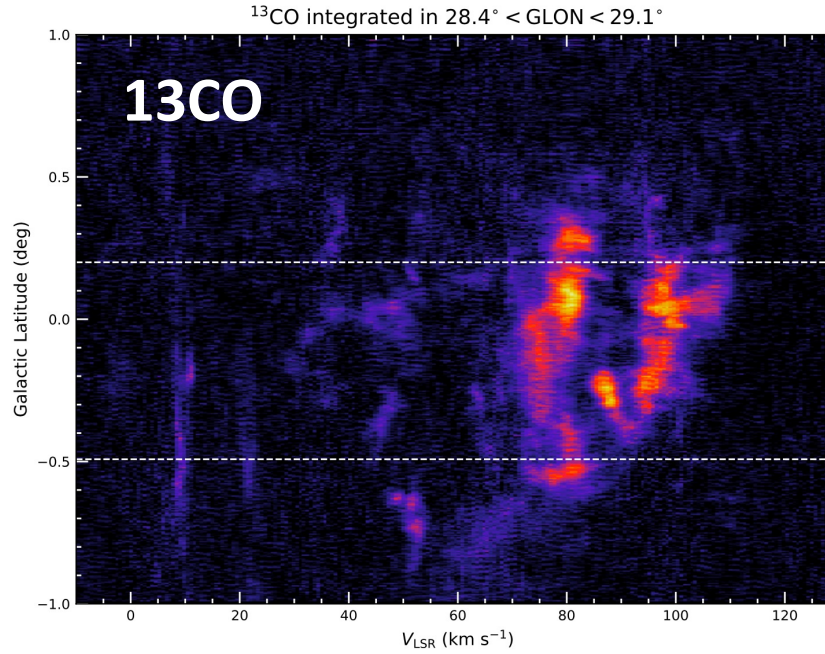
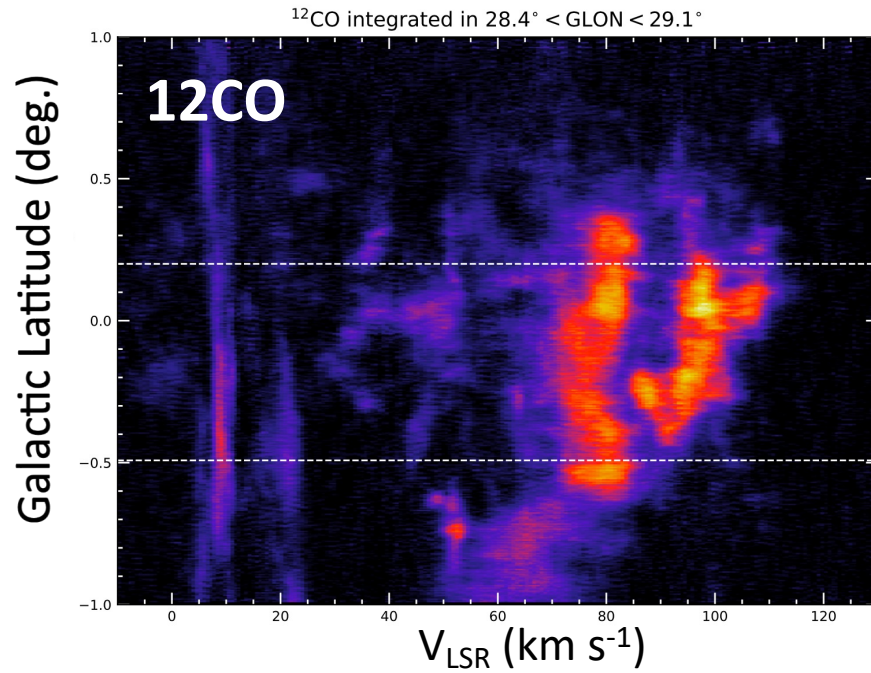
Galactic Longitude (deg.)



29.0

Comparison b/w ^{12}CO , ^{13}CO and C^{18}O

VLSR-GLON



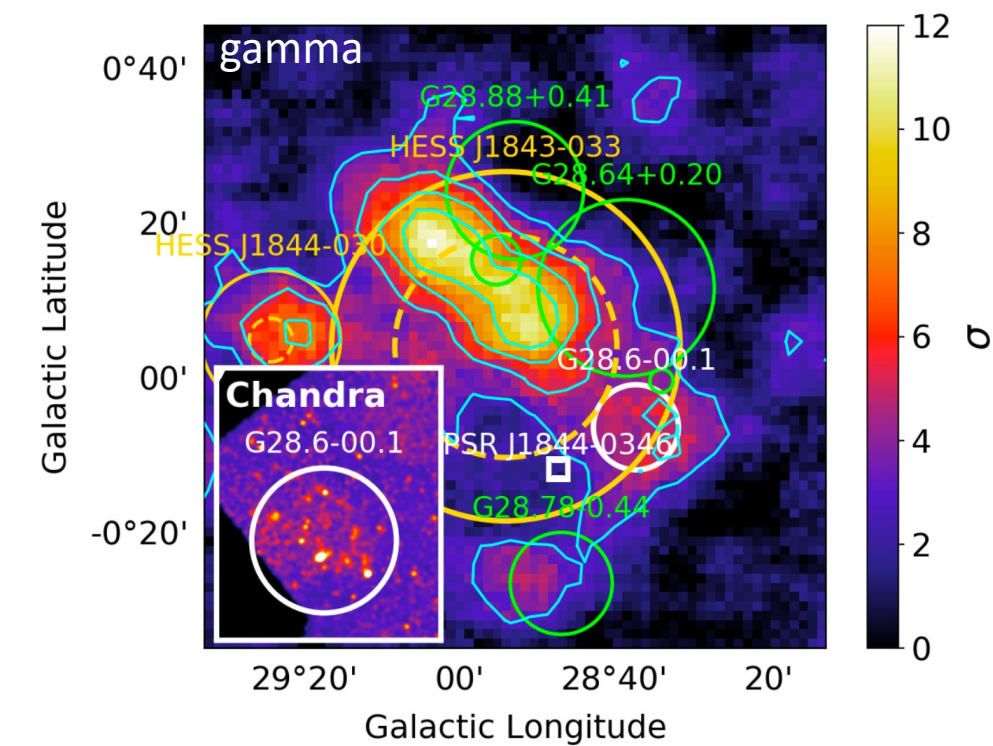
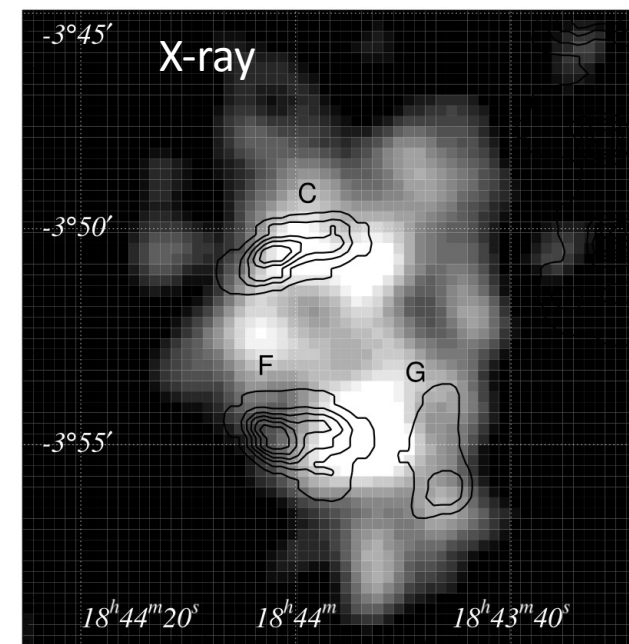
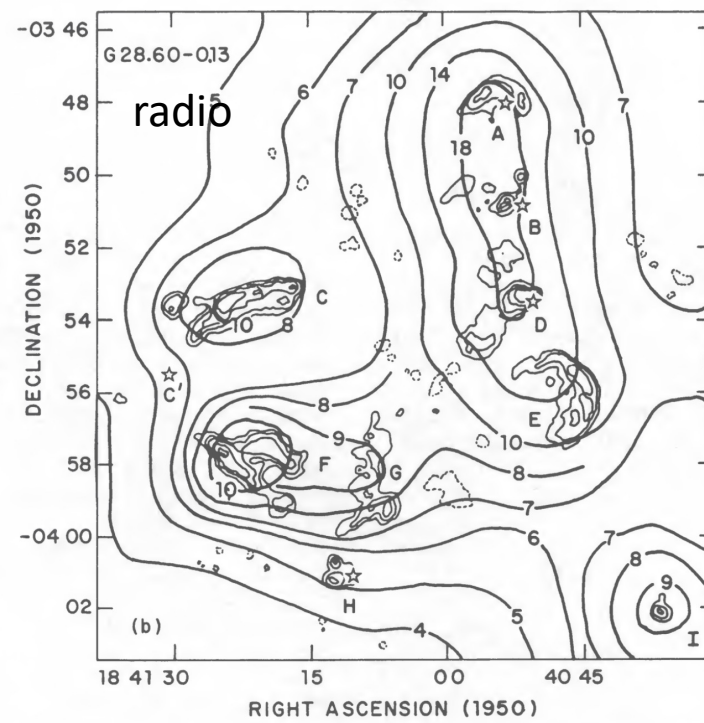
Modeling the gamma-ray emission (hadronic scenario)

SNR G28.6-0.1

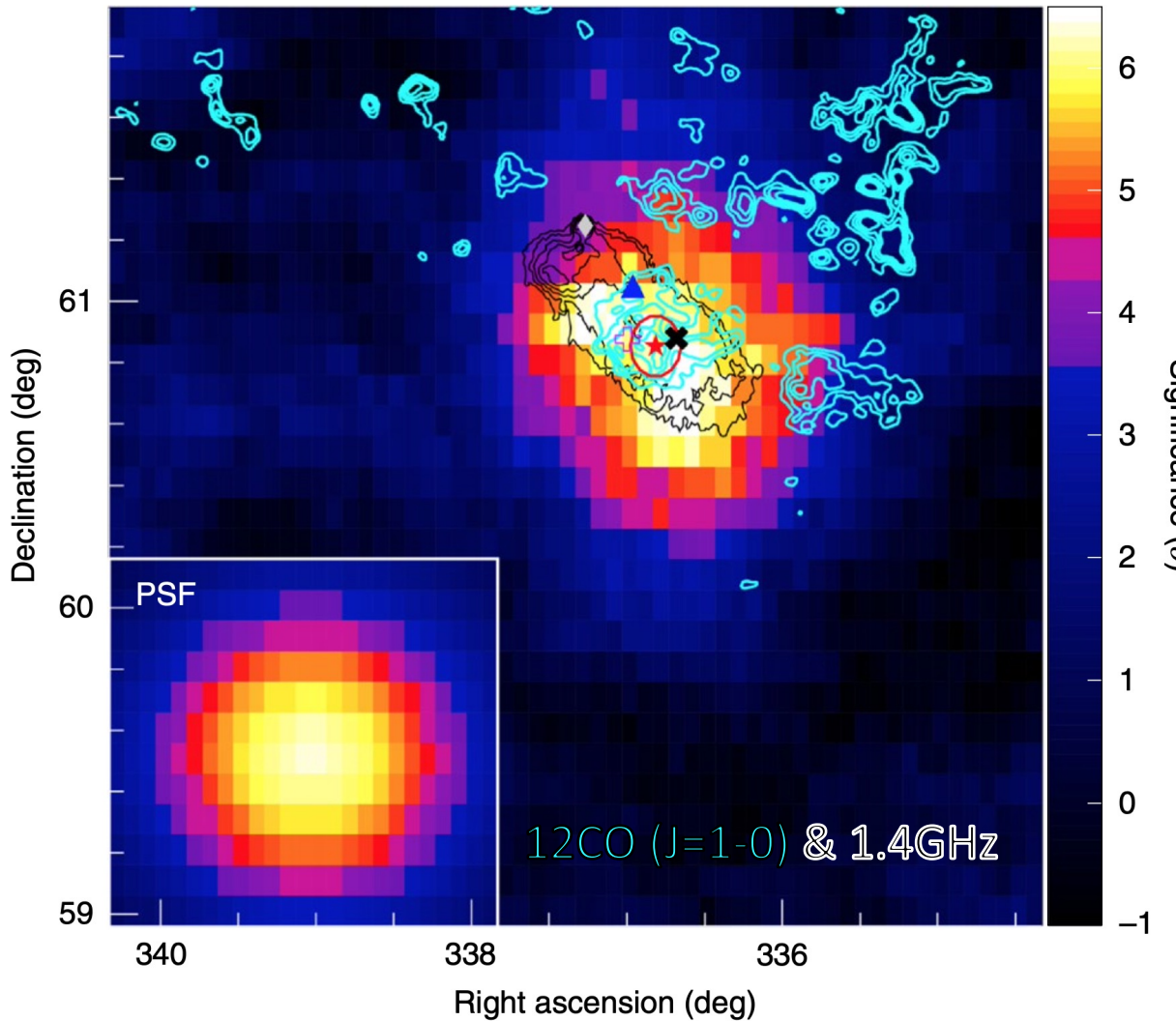
distance: 7 kpc (Bamba et al 2001), 9.6 ± 0.3 kpc (Ranasinghe and Leahy 2018)

age: 2.7 kyr (Bamba et al 2001), 19 kyr (Ranasinghe and Leahy 2018)

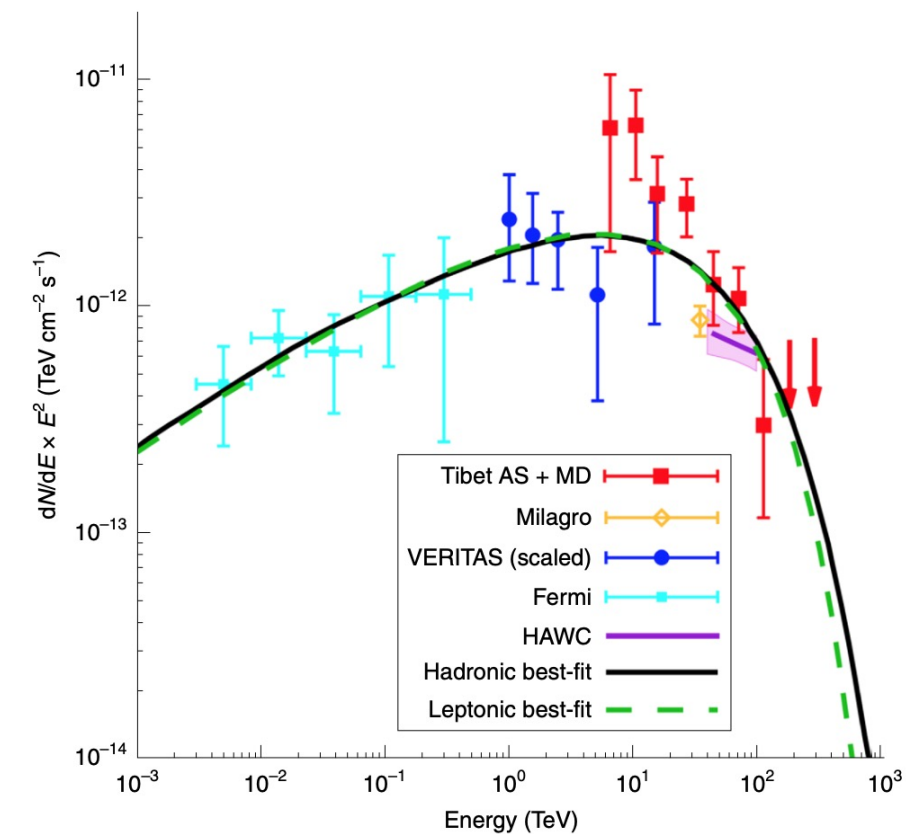
Non-thermal radio & X (Helfand et al 1989 & Bamba et al 2003) & TeV gamma (Devin et al 2021) are observed



SNR G106.3+2.7: A PeVatron candidate (Amenomori et al., Nat. Astron. 5, 460 (2021))



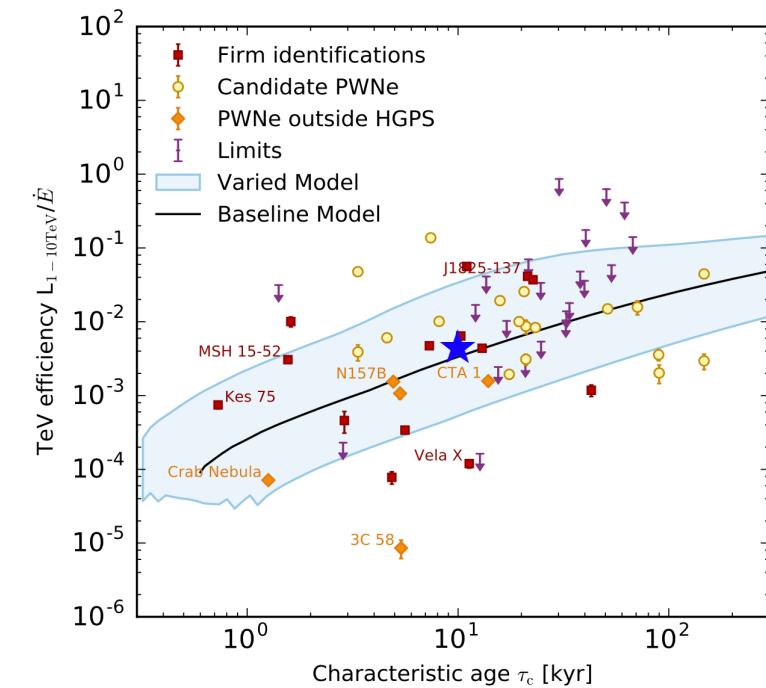
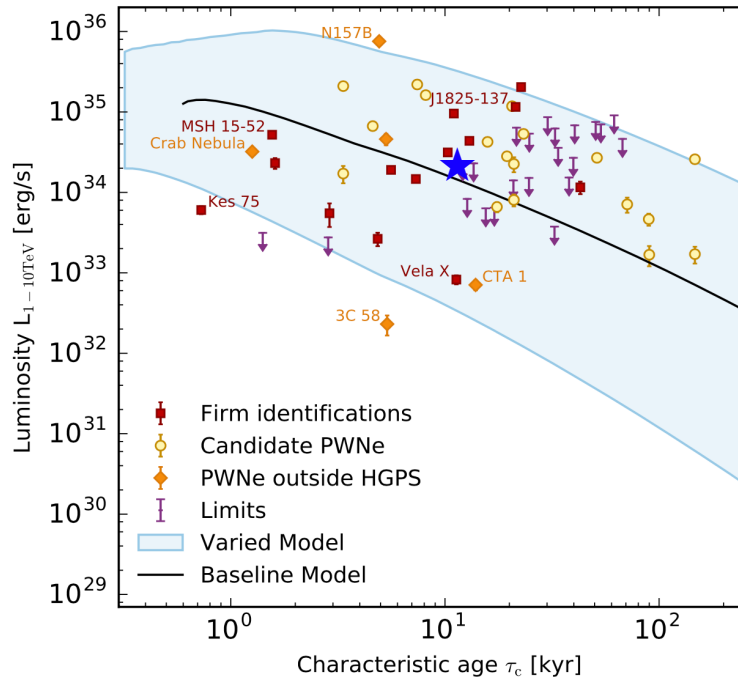
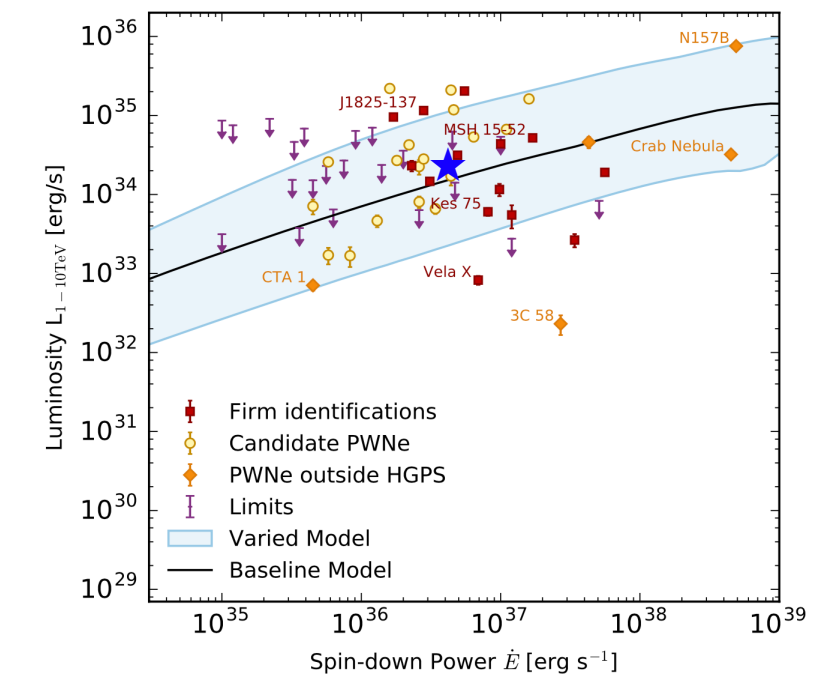
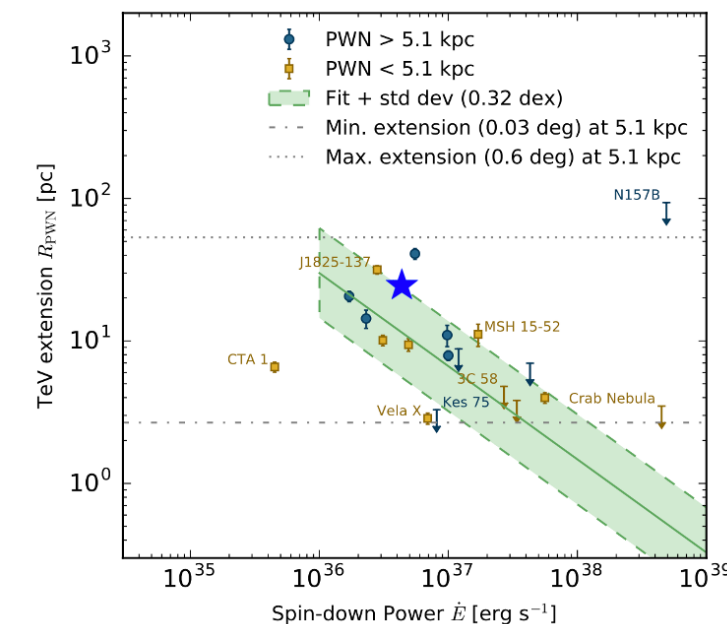
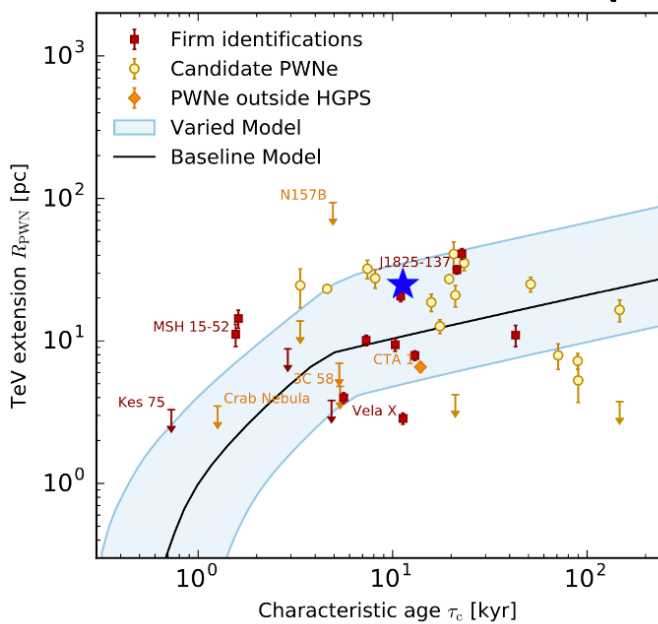
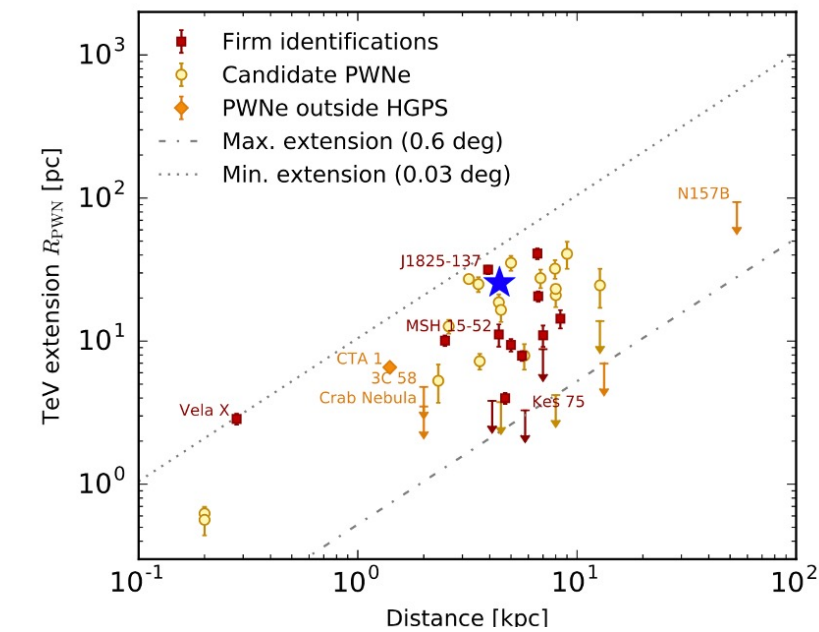
- age: ~ 10 kyr?
- distance: ~ 800 kpc?



	α	E_{cut} (TeV)	$W_{e/p}^\dagger$ (10^{47} erg)	B (μG)	χ^2/ndf
leptonic	$2.30^{+0.08}_{-0.07}$	190^{+127}_{-66}	$1.4^{+1.8}_{-0.7}$	$8.6^{+3.4}_{-2.5}$	12.8/15
hadronic	$1.79^{+0.08}_{-0.09}$	499^{+382}_{-180}	$5.0^{+0.7}_{-0.6}$	—	13.0/14

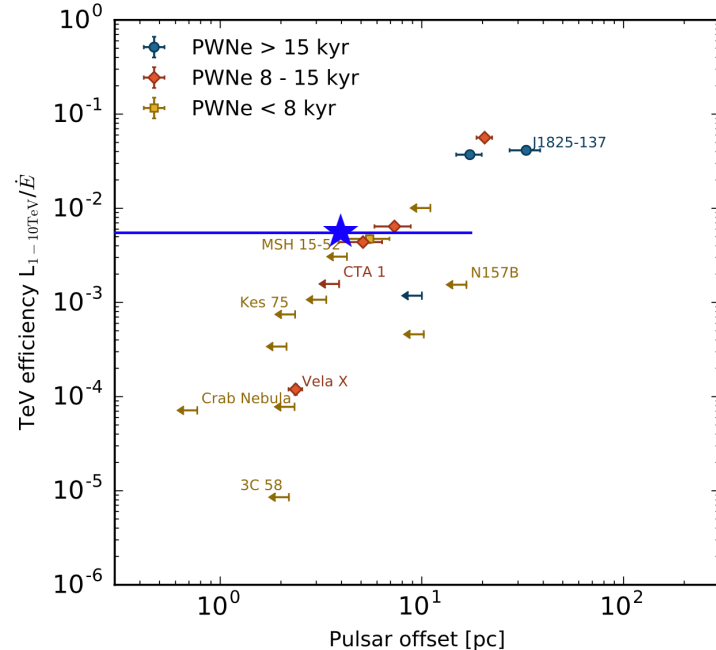
Association w/ PSR J1844-0346: TeV PWN?? (1)

H.E.S.S. collaboration, A&A 612, A2 (2018)

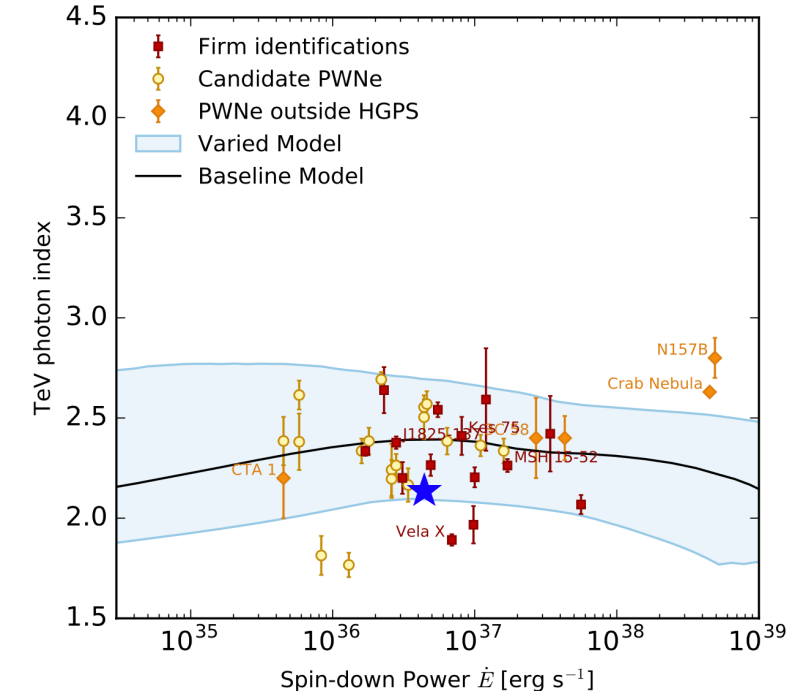
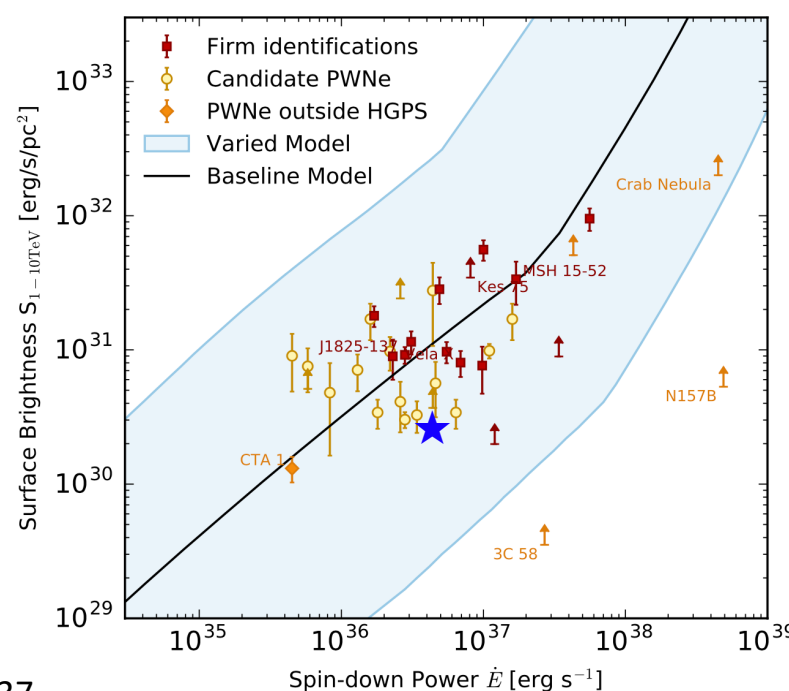


Association w/ PSR J1844-0346: TeV PWN?? (2)

H.E.S.S. collaboration, A&A 612, A2 (2018)



Error: Uncertainty on the position of TASG J1843-037



$$\text{Surface brightness} = \text{Luminosity} / (4\pi \times R_{\text{pwn}}^2) = 2.4 \times 10^{34} \text{ erg s}^{-1} / (4\pi \times 26 \text{ pc}^2) = 2.8 \times 10^{30} \text{ erg s}^{-1} \text{ pc}^{-2}$$

Photon index: 2.15 (H.E.S.S. collaboration, A&A 612, A1, 2018) or 2.02 from our result on the ECPL fit

Statistical research on PWNe

H.E.S.S. collaboration, A&A 612, A2 (2018)

Firm identification:

Table 1. HGPS sources considered as firmly identified pulsar wind nebulae in this paper.

HGPS name	ATNF name	Canonical name	$\lg \dot{E}$	τ_c (kyr)	d (kpc)	PSR offset (pc)	Γ	R_{PWN} (pc)	$L_{1-10\text{TeV}}$ ($10^{33} \text{ erg s}^{-1}$)
J1813-178 ¹	J1813-1749		37.75	5.60	4.70	<2	2.07 ± 0.05	4.0 ± 0.3	19.0 ± 1.5
J1833-105	J1833-1034	G21.5-0.9 ²	37.53	4.85	4.10	<2	2.42 ± 0.19	<4	2.6 ± 0.5
J1514-591	B1509-58	MSH 15-52 ³	37.23	1.56	4.40	<4	2.26 ± 0.03	11.1 ± 2.0	52.1 ± 1.8
J1930+188	J1930+1852	G54.1+0.3 ⁴	37.08	2.89	7.00	<10	2.6 ± 0.3	<9	5.5 ± 1.8
J1420-607	J1420-6048	Kookaburra (K2) ⁵	37.00	13.0	5.61	5.1 ± 1.2	2.20 ± 0.05	7.9 ± 0.6	44 ± 3
J1849-000	J1849-0001	IGR J18490-0000 ⁶	36.99	42.9	7.00	<10	1.97 ± 0.09	11.0 ± 1.9	12 ± 2
J1846-029	J1846-0258	Kes 75 ²	36.91	0.728	5.80	<2	2.41 ± 0.09	<3	6.0 ± 0.7
J0835-455	B0833-45	Vela X ⁷	36.84	11.3	0.280	2.37 ± 0.18	1.89 ± 0.03	2.9 ± 0.3	$0.83 \pm 0.11^*$
J1837-069 ⁸	J1838-0655		36.74	22.7	6.60	17 ± 3	2.54 ± 0.04	41 ± 4	204 ± 8
J1418-609	J1418-6058	Kookaburra (Rabbit) ⁵	36.69	10.3	5.00	7.3 ± 1.5	2.26 ± 0.05	9.4 ± 0.9	31 ± 3
J1356-645 ⁹	J1357-6429		36.49	7.31	2.50	5.5 ± 1.4	2.20 ± 0.08	10.1 ± 0.9	14.7 ± 1.4
J1825-137 ¹⁰	E1823-13		36.45	21.4	3.93	33 ± 6	2.38 ± 0.03	32 ± 2	116 ± 4
J1119-614	J1119-6127	G292.2-0.5 ¹¹	36.36	1.61	8.40	<11	2.64 ± 0.12	14 ± 2	23 ± 4
J1303-631 ¹²	J1301-6305		36.23	11.0	6.65	20.5 ± 1.8	2.33 ± 0.02	20.6 ± 1.7	96 ± 5

Counterpart?: eHWC J1850+001 abv. 56 TeV & LHAASO J1849-0003 @100 TeV

PWNe outside HGPS (firmly identified):

Table 3. Pulsar wind nebulae outside the HGPS catalogue.

Canonical name	ATNF name	$\lg \dot{E}$	τ_c (kyr)	d (kpc)	PSR offset (pc)	Γ	R_{PWN} (pc)	$L_{1-10\text{TeV}}$ ($10^{33} \text{ erg s}^{-1}$)
N157B ¹	J0537-6910	38.69	4.93	53.7	<22	2.80 ± 0.10	<94	760 ± 80
Crab Nebula ²	B0531+21	38.65	1.26	2.00	<0.8	2.63 ± 0.02	<3	32.1 ± 0.7
G0.9+0.1 ³	J1747-2809	37.63	5.31	13.3	<3	2.40 ± 0.11	<7	46 ± 7
3C 58 ⁴	J0205+6449	37.43	5.37	2.00	<2	2.4 ± 0.2	<5	0.23 ± 0.06
CTA 1 ⁵	J0007+7303	35.65	13.9	1.40	<4	2.2 ± 0.2	6.6 ± 0.5	0.71 ± 0.10

Candidate PWNe: Other than firmly identified PWNe, safisfy $\dot{E} / d^2 > 10^{34} \text{ erg s}^{-1} \text{ kpc}^{-2}$ & $\theta_{\text{PSR-TeV}} < 0.5 \text{ deg}$ & $\tau_c < 10^7 \text{ yr}$.

This list includes HESS J1908+063 for which eHWC J1907+063 and LHAASO J1908+0621 can be a counterpart.

Limits: PRSs (w/ $\dot{E} > 10^{35} \text{ erg s}^{-1}$) that coincide w/ a firm PWN HGPS src. or do not have a nearby HGPS src.

This list includes HESS J1841-055 for which eHWC J1839-057 and LHAASO J1839-0545 can be a counterpart.

